

**Glucose Transporter Expression and Regulation Following a Fast
in the Ruby-throated Hummingbird, *Archilochus colubris*.**

Raafay S. Ali^{1,2}, Morag F. Dick², Saad Muhammad^{1,2}, Dylan Sarver³, Lily Hou², G. William Wong³, and Kenneth C. Welch Jr.^{1,2}

¹ Cell and Systems Biology, University of Toronto, 25 Harbord St, Toronto, ON, Canada M5S 3G5

² Department of Biological Sciences, University of Toronto Scarborough Campus, 1265 Military Trail, Toronto, ON, Canada, M1C 1A4

³ Department of Physiology, Johns Hopkins School University School of Medicine, 725 North Wolfe Street Physiology 202, Baltimore, MD, United States of America, 21205

Corresponding author email: kenneth.welchjr@utoronto.ca

Keywords: hummingbird, glucose transporter, plasma membrane, glucose, fructose

Summary statement: Hummingbird ingest nectar rich in glucose and fructose. When fasted, tissue capacity for circulating glucose import declines while remaining elevated for fructose. This may underlie maintenance of high blood glucose and rapid depletion of blood fructose.

Abstract

Hummingbirds, subsisting almost exclusively on nectar sugar, face extreme challenges to blood sugar regulation. The capacity for transmembrane sugar transport is mediated by the activity of facilitative glucose transporters (GLUTs) and their localisation to the plasma membrane (PM). In this study, we determined the relative protein abundance of GLUT1, GLUT2, GLUT3, and GLUT5 via immunoblot using custom antibodies in whole-tissue and PM fractions of flight-muscle, heart, and liver of ruby-throated hummingbirds (*Archilochus colubris*). GLUTs examined were detected in nearly all tissues tested. Hepatic GLUT1 was minimally present in whole-tissue and absent in PM fractions. GLUT5 was expressed in flight-muscles at levels comparable to that of their liver, consistent with hummingbird flight-muscles' hypothesised uniquely high fructose-uptake and oxidation capacity. To assess GLUT regulation, we fed ruby-throated hummingbirds 1M sucrose *ad libitum* for 24 hours followed by either 1 hour of fasting or continued feeding until sampling. We measured relative GLUT abundance and concentrations of circulating sugars. Blood fructose concentration in fasted hummingbirds declined (~5 mM to ~0.18 mM), while fructose-transporting GLUT2 and GLUT5 abundance did not change in PM fractions. Blood glucose concentrations remained elevated in fed and fasted hummingbirds (~30 mM), while glucose-transporting GLUT1 and GLUT3 in flight muscle and liver PM fractions, respectively, declined in fasted birds. Our results suggest that glucose uptake capacity is dynamically reduced in response to fasting, allowing for maintenance of elevated blood glucose levels, while fructose uptake capacity remains constitutively elevated promoting depletion of blood total fructose within the first hour of a fast.

List of Abbreviations

AIC Akaike Information Criterion

AICc Akaike Information Criterion for small sample sizes

ANOVA Analysis of Variance

APS Ammonium Persulfate

cDNA Complementary Deoxyribonucleic Acid

CO₂ Carbon Dioxide

DTT Dithiothreitol

f_{exo} Proportion of expired CO₂ fuelled by oxidation of exogenous sugar

GAPDH Glyceraldehyde-3-Phosphate Dehydrogenase

GLUT Glucose Transporter

HEK293T Homo sapiens Embryonic Kidney cell line with Mutant SV40 large T antigen

HRP Horseradish Peroxidase

LC MRM/MS Liquid Chromatography Multiple Reaction Monitoring Mass Spectrometry

LMM Linear Mixed-effects Model

mM Millimolar

mRNA Messenger Ribonucleic Acid

MW Molecular Weight

NCBI National Center for Biotechnology Information

NP-40 Nonidet P-40

PBST Phosphate Buffered Saline with Tween 20

PM(F) Plasma Membrane (Fraction)

PVDF Polyvinylidene Fluoride

QQ plot Quantile-quantile plot

RIPA Radioimmunoprecipitation Assay

SDS Sodium Dodecyl Sulfate

SDS PAGE Sodium Dodecyl Sulfate Polyacrylamide Gel Electrophoresis

TEMED Tetramethylethylenediamine

TMIC The Metabolomics Innovation Centre

UTSC University of Toronto Scarborough Campus

WTH Whole Tissue Homogenate

Introduction

Hummingbirds primarily subsist on a diet of floral nectar high in sucrose, glucose, and fructose (del Rio et al., 1992). They are capable of oxidising glucose, fructose, or both, to power their characteristic hovering behaviour (Chen and Welch, 2014). When blood sugar concentrations are elevated, hummingbirds rely exclusively on these exogenous sugars to fuel nearly all the metabolic needs of their active cells (Welch et al., 2018). As such, they exhibit remarkable adaptations that enhance both the capacity for immediate rapid uptake and metabolism and the long-term storage of these sugars (Price et al., 2015; Welch et al., 2018). As they enter circulation, a proportion of ingested sugars are incorporated into hummingbirds' fat stores through *de-novo* lipogenesis by their liver (Suarez et al., 1988). When hummingbirds enter periods of hypoglycaemia, such as sleeping or fasted states, the entirety of their metabolic fuel source switches from circulating sugars to triglycerides derived from these fatty-acid stores (Eberts et al., 2019; Suarez et al., 1990). This switch is rapid, and a transition back to sugar metabolism occurs within a few minutes of sugar ingestion (Suarez and Welch, 2017). Furthermore, the switch from reliance on lipid oxidation to carbohydrate oxidation is nearly complete, such that mixed fuel-use does not occur for very long in hummingbirds with access to sufficient floral nectar (Welch et al., 2018).

Hummingbird digestive physiology, much like that of other nectarivores such as bats, facilitates rapid sugar transport across the intestinal lumen and into circulation (Karasov, 2017; Rodriguez-Peña et al., 2016). A high cardiac output and capillary-to-muscle-fibre ratio ensures high transport capacity of sugars to the site of active cells (Mathieu-Costello et al., 1992; Suarez, 1992). Sugars are then facilitatively imported across the plasma membrane (PM) of active cells (Suarez and Welch, 2011). Here, *in-vitro* studies of hummingbird muscle cells have demonstrated that the phosphorylation capacity of cytosolic kinases for glucose appears sufficient in providing energy for sustained hovering, although this may not be true for fructose (Myrka and Welch, 2018). As both delivery to and phosphorylation of glucose within muscles operate at rates near the theoretical maximum in vertebrates (Suarez et al., 1988; Suarez and Welch, 2017) it is likely that regulation at the site of import itself exerts a great deal of control over the flux through the entirety of the sugar oxidation cascade. Along with delivery and phosphorylation, the sugar import step is a rate-limiting process in the paradigm outlined by Wasserman et al. (2011) and is nearly entirely dependent on the presence and distribution of

active glucose transporters (GLUTs) (Wasserman, 2009). These proteins are a family of transmembrane solute transporters (Mueckler and Thorens, 2013). While expression of certain GLUT isoforms have been demonstrated in a variety of avian species (Coudert et al., 2018; Hussar et al., 2019; Sweazea and Braun, 2006), including hummingbirds (Myrka and Welch, 2018; Welch et al., 2013), the study of avian GLUT regulation has been limited to cell-based approaches (Steane et al., 1998; Wagstaff and White, 1995; Yamada et al., 1983). In this study, we further characterised GLUT isoform expression and sought to understand *in vivo* GLUT regulation in hummingbirds.

Studies of mammalian GLUTs demonstrate that their expression in the PM is regulated by a variety of intra- and extracellular factors, including blood sugar and insulin concentrations, exercise, and stress (Egert et al., 1999; Guma et al., 1995; Yang and Holman, 1993). The expression and functional distribution and regulation of hummingbird GLUTs, however, remains relatively unknown. Studies on GLUT isoforms of the closest relatively well-examined avian species, the chicken (*Gallus gallus domesticus*), are fragmented and the distribution of avian GLUT isoforms is not fully understood (Byers et al., 2018; Suarez and Welch, 2011; Sweazea and Braun, 2006). It is known that chicken GLUT1 and GLUT3 share sequence homologies of ~80% and ~70%, respectively, with human GLUTs, but other isoforms such as GLUT2 and GLUT5 only share ~65% and ~64% sequence homology (calculated via NCBI BLAST (Boratyn et al., 2012), summarised in Table S6). It is also clear that they are regulated very differently in each class (Wagstaff and White, 1995; Yamada et al., 1983). Despite this, the literature on mammalian GLUTs provides a useful foundation for understanding the affinities and ligand-specificity of avian, including hummingbird, GLUTs. In mammals, GLUT3, followed by GLUT1, show the highest affinities for glucose; $K_m \approx 1.5$ mM (Thorens and Mueckler, 2010) and $K_m \approx 3-5$ mM (Zhao and Keating, 2007), respectively. GLUT5 transports fructose ($K_m \approx 11-12$ mM; Douard and Ferraris, 2008), and is largely found in mammalian enteric and renal tissue (Douard and Ferraris, 2008), although some presence in hepatic tissue has also been noted (Godoy et al., 2006; Zhao et al., 1993). GLUT2, uniquely, shows affinity for both sugars. While its affinity for glucose and fructose ($K_m \approx 17$ mM and $K_m \approx 76$ mM, respectively; Zhao and Keating, 2007) is relatively low compared to other isoforms, it plays a dominant role in hepatic sugar transport (Wood and Trayhurn, 2003).

Importantly, it is only when GLUT isoforms are expressed and active in the PM that transmembrane sugar transport can occur from the blood into the active cell (Guma et al., 1995; Wasserman, 2009; Yamada et al., 1983). In mammals, GLUT4 translocation to the PM by insulin-stimulation following feeding is known to recruit other GLUT isoforms to the PM as well, increasing the sugar import rate into active cells (Guma et al., 1995). Hummingbirds (Welch et al., 2013), much like chickens (Byers et al., 2018), do not express transcript or protein of the insulin-sensitive GLUT4 isoform. Chicken insulin levels do not significantly change with dietary status (Simon et al., 2011), and this is presumably also true in hummingbirds. Further, circulating insulin does not significantly increase sugar import in chicken muscles (Chen, 1945), though it may in the liver (Dupont, 2009; Zhang et al., 2013). Lastly, and unlike mammals, hummingbirds have limited intramuscular glycogen stores (Suarez et al., 1990), and therefore rely on newly imported sugars from circulation for carbohydrate oxidation (Welch et al., 2018). Despite missing critical elements of the insulin-GLUT4 pathway, fed hummingbirds utilise circulating sugars, when available, at very high rates to meet their metabolic demands (Suarez and Welch, 2017).

Previous studies have confirmed the presence of GLUT1 and GLUT5 transcript in nearly all hummingbird tissue examined (Myrka and Welch, 2018). Immunohistochemistry of hummingbird myocytes using a commercial antibody for GLUT1 have also shown GLUT1 localisation to the PM (Welch et al., 2013), though, the results were not definitive. In this study, using custom antibodies for the different isoforms of hummingbird GLUTs, we sought to identify the tissue-specific protein distribution and to quantify the abundance in the PM, of GLUT1, GLUT2, GLUT3, and GLUT5. We predicted GLUT1 would be detected in hummingbird flight muscle, cardiac, and liver tissue, in accordance with its ubiquitous presence in mammalian tissue (Mueckler and Thorens, 2013), as well as its previous detection in hummingbird myocytes (Welch et al., 2013). As GLUT2 plays a stronger role in enteric (Karasov, 2017) and hepatic (Mueckler and Thorens, 2013) sugar transport, we predicted that its abundance would be limited in muscles and more predominantly found in the liver. In mammals, GLUT3 is observed in close association with GLUT1 (Simpson et al., 2008) and may function as a replacement for GLUT4 in certain muscle developmental stages (Klip et al., 1996). We expected to detect GLUT3 in tissues also expressing GLUT1. We also expected to find GLUT5 in both the liver and muscles, as hummingbird muscles are capable of supporting hovering flight

on fructose-only meals (Chen and Welch, 2014). To further characterise the regulatory aspects of hummingbird GLUTs, we compared the abundance of GLUT1, GLUT2, GLUT3, and GLUT5 in the PM of fed and fasted hummingbirds. We also measured levels of circulating glucose and fructose in these birds. Based on previous measurements of hummingbird blood glucose (Beuchat and Chong, 1998), we expected to see high blood glucose concentrations (~40 mM) in the fed condition and lower levels in the fasted (~15-25 mM). Previous measurements of hummingbird blood fructose have not been made. However, similar to that of frugivorous bats (Keegan, 1977), we predicted blood fructose concentrations in fed hummingbirds to be ~5-10 mM in fed and ~0 mM in fasted hummingbirds. Given the rapid switching between glucose or fructose oxidation and oxidation of lipid stores in foraging versus fasting hummingbirds, we expected a greater abundance of PM GLUT1, PM GLUT3, and PM GLUT5 in flight muscle and liver of fasted hummingbirds. Finally, we expected little difference between GLUT2 abundance in the PM of tissue from fed and fasted hummingbirds.

Materials and Methods

1.1 Animal Use and Ethics Statement.

This study was approved and performed adhering to the requirements of the University of Toronto Laboratory Animal Care Committee and the Canadian Council on Animal Care. Twelve adult male ruby-throated hummingbirds (*Archilochus colubris*) were captured in the early summer at the University of Toronto Scarborough (UTSC) using modified box traps and housed individually in Eurocages (Corners Ltd, Kalamazoo, MI, USA) in the UTSC vivarium under a 12:12 hour light:dark cycle. They were provided with perches and fed on a maintenance diet of NEKTON-Nectar-Plus (Keltern, Germany) for 2-3 months until the start of the experiment.

All hummingbirds were provided with ~33% sucrose solution for 24 hours prior to the experiment. Birds were divided into a fed group (n = 6), which was provided with *ad-libitum* 1M sucrose solution up to sampling, beginning at 10AM, and a fasted group (n = 6), which was deprived of any food for a 1 hour duration prior to the 10AM sample collection. To minimize interindividual variation in activity level and energy expenditure, birds from both treatment groups were held in small glass jars, perched on wooden dowels, in which they were constrained from flying, for the duration of the 1 hour fast. Respirometry measurements by Chen and Welch

(2014) have previously shown that this is sufficient time for the fasted hummingbirds to shift from fuelling metabolism with circulating sugars to fats. Fed hummingbirds will continue to exclusively metabolise sugars. Hummingbirds were then anaesthetised with isofluorane inhalation and euthanized via decapitation. Immediately after decapitation, blood was sampled from the carotid artery using heparinized capillary tubes and spun at 3800 g for 10 minutes at room temperature and the plasma stored at -80°C . Flight muscle (the pectoralis and supracoracoideus muscles), heart, and liver were extracted and frozen with isopentane cooled with liquid nitrogen. All tissues were stored at -80°C .

1.2 Circulating Sugar and Metabolite Analysis.

Plasma samples were sent to the Metabolomics Innovation Centre (TMIC) at the University of Victoria (Victoria, British Columbia, Canada) to be analyzed via service 45 (absolute quantitation of central carbon metabolism metabolites and fructose) found here: <https://www.metabolomicscentre.ca/service/45>. Quantitation of glucose and fructose concentrations in plasma samples was achieved via chemical derivatization – liquid chromatography – multiple reaction monitoring/mass spectrometry (LC-MRM/MS) following a protocol outlined by Han et al. (2016). Quantitation of central carbon metabolites (organic acids; lactate and pyruvate) of flight muscle was done via the protocol outlined by Han et al. (2013).

1.3 Antibody Design, Production, and Isoform Specificity

Anti-rabbit polyclonal antibodies for GLUT isoforms were designed in conjunction to minimise cross-reactivity using the services of Pacific Immunology (Ramona, CA, USA). Epitope design was accomplished using messenger RNA (mRNA) sequences for ruby-throated hummingbird GLUT isoforms 1, 2, 3, and 5 that were obtained from the hummingbird liver transcriptome (Workman et al., 2018) (Table S4). The concentration of the affinity-purified antibody samples was assessed using ELISA by Pacific Immunology (ab-GLUT1 $\approx 1.1 \text{ mg}\cdot\text{ml}^{-1}$, ab-GLUT2 $\approx 5.7 \text{ mg}\cdot\text{ml}^{-1}$, ab-GLUT3 $\approx 2.6 \text{ mg}\cdot\text{ml}^{-1}$, ab-GLUT5 $\approx 1.0 \text{ mg}\cdot\text{ml}^{-1}$). The final experimental dilutions were determined empirically through preliminary experiments and are provided below.

1.3.1 Generation of mammalian expression plasmids encoding *A. colubris* GLUT1, GLUT2, GLUT3, and GLUT5.

The cDNA encoding *A. colubris* GLUT1 (NCBI Accession Number MT472837), GLUT2 (MT472838), GLUT3 (MT472839), and GLUT5 (MT472840) were synthesized by GenScript

based on the full-length mRNA sequences derived from our previously published RNA sequencing data (Workman et al., 2018). The V5 epitope tag (encoding the peptide “GKPIP NPLLGLDST”) was inserted at the 3’ end of each cDNA immediately after the last coding amino acid. All epitope-tagged cDNA sequences were cloned into the EcoRI restriction site of the mammalian expression vector, pCDNA3.1 (+) (Invitrogen). All expression plasmids were verified by DNA sequencing.

1.3.2 Specificity immunoblots

SDS-PAGE was run on cell lysates of HEK293T cells transiently transfected, using lipofectamine 2000 (Invitrogen), with hummingbird GLUT1, GLUT2, GLUT3, or GLUT5 (acGLUT1, GLUT2, GLUT3, or GLUT5) expression vectors; all containing a V5 tag. Cell lysates produced using RIPA buffer (50 mM Tris-HCl, pH 7.4; 150 mM NaCl; 1 mM EDTA; 1% Triton X100; 0.25% deoxycholate) supplemented with protease and a phosphatase inhibitor cocktail (MilliporeSigma, Burlington, Massachusetts, USA and Roche, Basel, Switzerland; respectively). Each lysate was confirmed to express the appropriate recombinant protein at the expected size using an anti-V5 antibody produced in rabbit (Sigma V8137). Isoform specificity was tested via immunoblotting all cell lysates (empty vector control, acGLUT1, GLUT2, GLUT3, and GLUT5) with each novel acGLUT antibody and observing GLUT protein signal overlap; none was observed. Briefly, each immunoblot lane represents a cell lysate produced from an entire well of a 6-well cell-culture dish (Thermo Scientific, Nunc). Lysates were diluted with SDS loading dye (final concentration: 50 mM Tris-HCl, pH 7.4, 2% SDS, 6% glycerol, 1% 2-ME, and 0.01% bromophenol blue) and not boiled. An equal volume of each lysate was added to the designated lane on a 12% polyacrylamide gel (Bio-Rad, Hercules, CA, USA) and separated by electrophoresis. The BioRad Trans-Blot Turbo semidry system was used to transfer protein onto PVDF membranes. Blots were blocked in 5% non-fat milk in Phosphate buffered saline with Tween 20 (PBST) and exposed to primary antibodies overnight at 4°C. After washing, blots were exposed to HRP-conjugated secondary antibody (Anti-Rabbit IgG, 7074S, Cell Signaling Technology, Danvers, MA, USA) for 1 h at room temperature and developed in ECL (Amersham ECL Select; GE Healthcare, Chicago, IL, USA). Bands were visualized with the MultiImage III FluorChem Q (Alpha Innotech, San Leandro, CA, USA). Primary antibodies were diluted 1:1000 in PBST + 0.02% sodium azide. The secondary antibody was diluted 1:10,000 in PBST + 0.02% sodium azide.

1.4 Tissue Sample Preparation.

Each sample underwent either a plasma membrane fractionation protocol established by (Yamamoto et al., 2016) and slightly modified by replacing NP-40 (nonidet P-40) with Triton X-100 (Sigma-Aldrich, St. Louis, Missouri) to obtain only PM-proteins, or a radioimmunoprecipitation assay buffer (RIPA) homogenisation (part of the same protocol) to obtain all proteins contained in a whole-cell. Fractionation used different detergent concentrations (0.1%, 1%, 2%) in the homogenisation buffers to solubilise proteins and create protein-detergent complexes depending on whether they are in the hydrophilic (cytosolic) domain or the hydrophobic (PM) domain.

1.4.1 Buffer composition.

Buffer A01 (0.5 M DTT, ddH₂O, and 0.1% v/v Triton X-100), A1 (0.5 M DTT, ddH₂O, and 1% v/v Triton X-100), and 2× RIPA (20 mM Tris-HCl, pH 8.0, 300 mM NaCl, 2% v/v Triton X-100, 1% w/v sodium deoxycholate, 0.2% w/v sodium dodecyl sulfate (SDS), 1 mM DTT) were prepared. All reagents were cooled to 4°C before homogenisation and included Sigma P8340 protease inhibitor cocktail.

1.4.2 Homogenisation and plasma membrane fractionation.

20 mg of flight muscle, liver, or heart was cut on a cold aluminum block and immediately placed in an ice-bath. The tissue was minced in buffer A01 with scissors and homogenised using a VWR handheld pestle homogenizer (BELAF650000000). The homogenate was passed through a 21G needle three times to liberate nuclear and intracellular proteins. An aliquot of the homogenate was left on ice for 60 minutes in 2× RIPA buffer. This whole-tissue RIPA-fraction was then centrifuged at 12,000 g for 20 minutes at 4°C, allowing proteins to be solubilised. The supernatant was collected and stored at -80°C as the whole-tissue homogenate. The remainder of the homogenate was centrifuged at 200 g for 1 min at 4°C. The upper phase was set aside, and 90 µL of buffer A01 was added to the lower phase which was homogenised for 10 seconds. The lower phase was centrifuged at 200 g for 1 minute and added to the tube containing the upper phase. The combined phases were centrifuged at 750 g for 10 minutes. The supernatant consisting of non-PM proteins was removed. The remainder of the protein-detergent complexed pellet was resuspended with buffer A1 and kept on ice for 60 minutes. After centrifugation at

12000 g for 20 minutes, the supernatant containing only PM-associated proteins was collected as the “plasma membrane fraction”.

1.5 SDS-PAGE.

10% resolving and 4% stacking gels were cast using a 15-well comb and the AA-Hoefer Gel Caster Apparatus (10%; 33% 30%-Acrylamide (37.1:1), 33% Separating gel buffer (1.5 M Tris Cl, 0.4% SDS), 55% ddH₂O, 0.65% ammonium persulfate (APS), 5.5% TEMED), (4%; 13.4% 30%-Acrylamide, 9.3% Stacking gel buffer (0.5 M Tris Cl, 0.4% SDS), 33% ddH₂O, 0.06% APS, 3.3% TEMED). Samples were incubated in a 1:1 (w/v) ratio of 2× sample buffer (0.2 M DTT, BioRad Laemmli Sample Buffer #1610737) at room temperature for 20 minutes. The AA-Hoefer SE600 Vertical Gel Electrophoresis apparatus was set up with 6 L running buffer (10% BioRad 10× Tris/Glycine/SDS #1610732, 90% ddH₂O). The gel was run at 90 V for 20 minutes and 110 V for another 75 minutes with power supplied from an AA-Hoefer PS200HC Power Unit.

1.5.1 Electroblot and immunoblot

The SDS-PAGE gel was transferred to 0.45 μm pore nitrocellulose (NC) membrane (GE Life Sciences #10600003 Protran Premium 0.45 NC) using the AA-Hoefer TE22 Mighty Small Transfer unit at 110 V for 90 minutes with water cooling and immersion in an icebath. The transfer buffer consisted of 192 mM glycine, 24.8 mM Tris, 0.00031% SDS, 20% methanol. To normalise, a total-protein stain, SYPRO Ruby Red Blot (BioRad #1703127), was used and imaged on a Bio-Rad PharosFX Molecular Imager (#1709460) using a 532 nm laser and captured with a 600-630 nm band pass filter. The membranes were incubated with primary antibody overnight at the following dilutions in PBST (phosphate-buffered saline, 0.1% Tween-20) buffer: GLUT1 (1:250), GLUT2 (1:2000), GLUT3 (1:2000), GLUT5 (1:500). Membranes were then incubated with anti-rabbit horseradish-peroxidase-conjugated secondary antibody (Cell Signalling Technology #7074) at 1:1000 dilution with PBST. Finally, Pierce Electrochemiluminescent Reagent (Pierce 32106) was used to fluoresce conjugates which were imaged using a BioRad Chemidock XRS+ Gel Imager.

1.6 PM fraction purity

To validate the separation of PM proteins from cytosolic proteins, commercially available control antibodies were used that were validated by the manufacturer for cross-reactivity in

chickens. Known PM-residing and cytosol-residing proteins targeted and their abundance was used to assess the degree of PM fractionation in flight muscle, liver, and heart samples. The membranes were incubated at 1:1000 dilution for 90 minutes at room temperature and included antibodies for 1) E-cadherin (Cell Signalling Tech. 24E10), 2) Na⁺/K⁺ ATPase (Cell Signalling Tech. 3010), 3) Glyceraldehyde-3-phosphate dehydrogenase (GAPDH) (Cell Signalling Tech. 14C10), and 4) Fatty acid translocase (FAT) (Abgent AP2883c) (summarised in Table S2).

1.7 Western Blot Band Normalisation.

GLUT protein molecular weights were predicted using ExPASy (Gasteiger et al., 2005). Protein quantitation was done with a Pierce 660 nm assay. 5µg of sample protein was loaded into each well of the polyacrylamide gel, in comparison with wells containing visible protein ladder (Sigma 26616). The antibody staining intensity of each Western blot sample was normalised to its corresponding total-protein stain intensity using BioRad ImageLab software. Background subtraction was applied to the total protein stain in a lane-wise fashion, while no background subtraction was applied to the antibody staining intensity. Fluorescence intensity for the total-protein stain was measured using 30% of the lane-width as per the recommendation of Gassmann et al. (2009). The antibody stain was measured using a fixed lane-width comprising of the entire lane. Normalised molecular weights were recorded.

1.8 Statistical Analysis.

A Student's T-test was performed for the sugar and metabolite concentrations between fed and fasted hummingbirds. We evaluated variation in isoform intensity data for each GLUT by creating linear mixed-effects models (LMMs) in R statistical language (version 3.6.1, r-project.org) using the lme4 package (Bates et al., 2015) for GLUT isoform fluorescence intensity data. We compared relative GLUT 1, 2, 3, and 5 abundance among tissues, and between fed and fasted individuals using a fully factorial design. Assumptions of residual normality were checked through visual inspection of the quantile-quantile (Q-Q) plot, a frequency histogram, and the Shapiro-Wilk Normality Test. When necessary, model parameters were transformed by a chosen function (the details of which are presented in the Results section below) resulting in the greatest homoskedasticity. The data was fitted using the following formula:

$$\text{Fluorescence Intensity} \sim \text{Treatment} \times \text{Tissue} + \text{Blot}$$

which outperformed more simplified models, as indicated by AICc (Akaike information criterion corrected for small sample sizes), the details of which are presented in Table S5. To account for the contribution of blot-to-blot variation, individual blots were treated as random effects (represented as *Blot* in the formula). Analysis of variance (ANOVA) was performed on the model parameters to determine the significance of any interactions. Post-hoc analysis was performed using the emmeans package (Lenth, 2019) within R software to determine group means and standard error. Pairwise comparison was performed to determine statistical significance of groups using the Tukey HSD method with the contrast function from the emmeans package. All data are presented as mean \pm standard error.

Results

2.1 Circulating Sugars and Metabolites of Fed and Fasted Hummingbirds

Overall, plasma samples demonstrated a significant difference for only blood fructose concentrations ($t_{9,9} = -17.2$, $p = 0.001$) which were higher in fed hummingbirds (5.34 ± 0.2 mM) compared to fasted (0.21 ± 0.1 mM). Glucose concentrations in fed hummingbirds (30.04 ± 2.0 mM) remained similarly elevated in fasted hummingbirds (29.67 ± 1.5 mM). Flight muscle homogenates indicated that lactate concentrations in fed individuals (4.31 ± 1.3 mM) were slightly lower than in fasted (6.35 ± 0.9 mM) although this was not a significant difference. Likewise, pyruvate concentrations in fed hummingbirds (0.21 ± 0.03 mM) remained elevated in fasted hummingbirds (0.22 ± 0.01 mM). These results are summarised in Figure 1.

2.2 Antibody Specificity and GLUT Detection

Antibodies showed a high degree of specificity for their isoform in immunoblots of HEK293 cell lysates (Table S3). In hummingbird tissue, GLUT proteins were identified by band molecular weights, and were, with one exception, present in both PM fractions and whole-tissue homogenates following PM fractionation (Table S1). GLUT1, GLUT2, GLUT3, and GLUT5 were detected in whole-tissue homogenates of flight muscle and heart tissue of ruby-throated hummingbirds, as well as in PM fractions. GLUT1 in liver whole-tissue homogenates was minimally detected and was not detected at all in liver PM fractions. GLUT1, GLUT2, and GLUT5 were detected at approximately their expected molecular weights in all tissues. GLUT3 was detected at a size slightly larger than predicted.

2.3 Relative GLUT Abundance

2.3.1 GLUT1

Flight muscle whole-tissue, regardless of treatment, had a similar GLUT1 abundance to heart whole-tissue. However, flight muscle whole-tissue had significantly greater GLUT1 abundance compared to liver whole-tissue in both fed (flight muscle / liver ratio: 4.75 ± 1.27 , $t_{3,02} = 4.54$, $p = 0.040$) and fasted (flight muscle / liver ratio: 5.76 ± 1.54 , $t_{3,02} = 4.28$, $p = 0.046$) individuals. These results are summarised in Table 3 and Fig. 2A. The treatment, fasting, had a significant effect on GLUT1 abundance in whole-tissue homogenates ($F_{1,13} = 7.99$, $p = 0.014$). Post-hoc analysis, however, revealed that only flight muscle whole-tissue GLUT1 abundance was

significantly lower in fasted hummingbirds (fasted/fed ratio: 0.73 ± 0.09 ; $t_{13} = 2.63$, $p = 0.021$) (Table 1).

With respect to PM fractions, we observed a significant effect of tissue ($F_{1, 3.78} = 24$, $p = 0.009$) and the interaction of tissue and treatment ($F_{1, 13.02} = 17.03$, $p = 0.012$). Multiple comparisons revealed that the relative abundance of PM GLUT1 was >2-fold higher in flight muscle PM fractions compared to heart PM fractions only in the fed condition (Fed flight muscle / fed heart ratio: 4.87 ± 1.31 , $t_{4.68} = 5.89$, $p = 0.009$). These results are summarised in Table 4 and Fig. 2B. Additionally, PM GLUT1 abundance was significantly lower in-flight muscle PM fractions of fasted hummingbirds (fasted/fed ratio: 0.61 ± 0.06 , $t_{13} = 4.66$, $p = 0.002$) (Table 2).

2.3.2 GLUT2

No significant difference was observed among whole-tissue homogenates in their relative GLUT2 abundance regardless of treatment (Table 3). However, a significant effect of fasting treatment was observed among whole-tissue homogenates ($F_{1, 11} = 6.22$, $p = 0.029$). Multiple comparisons revealed that only flight muscle whole-tissue had a significantly lower relative GLUT2 abundance in fasted hummingbirds (fasted/fed ratio: 0.54 ± 0.08 , $t_{14.5} = 2.63$, $p = 0.019$). Heart whole-tissue and liver whole-tissue did not show a significant difference in GLUT2 abundance with fasting treatment (Table 1 and Fig. 3A).

PM fractions did not show any significant difference among tissues, treatment, or the interaction of tissue and treatment for GLUT2 relative abundance (Table 2, Table 4, and Fig. 3B).

2.3.3 GLUT3

Relative GLUT3 abundance among whole-tissue homogenates was similar regardless of treatment with one exception: liver whole-tissue had significantly greater GLUT3 abundance compared to heart in fed individuals (fed liver / fed heart ratio: 2.46 ± 0.46 , $t_{3.5} = 5.83$, $p = 0.014$) (Table 3 and Fig. 4B). The treatment, fasting, significantly affected the whole-tissue relative abundance of GLUT3 ($F_{1, 11} = 17.08$, $p = 0.002$). Post-hoc analysis revealed that both flight muscle whole-tissue (fasted/fed ratio: 0.68 ± 0.09 , $t_{24.8} = 2.61$, $p = 0.015$) and liver whole-tissue (fasted/fed ratio: 0.58 ± 0.09 , $t_{24.8} = 4.58$, $p = 0.0001$) had significantly less GLUT3 in fasted individuals. No significant difference was observed in the GLUT3 relative abundance of heart whole-tissue (Table 1 and Fig. 4A).

In PM fractions, a significant effect of the fasting treatment was observed on the relative GLUT3 abundance ($F_{1,16} = 13.13$, $p = 0.002$). Through post-hoc analysis, we observed that GLUT3 relative abundance was significantly lower in only in liver PM fractions of fasted hummingbirds (fasted/fed ratio: 0.58 ± 0.14 , $t_{16} = 4.54$, $p = 0.004$) (Table 2). No significant difference was observed among tissues, however, the interaction of tissue and treatment was significant ($F_{2,16} = 6.46$, $p = 0.009$) (Table 4).

2.3.4 GLUT5

Among whole-tissue homogenates, no significant effect of tissue or treatment, or their interaction, were observed for the relative abundance of GLUT5. Regardless of treatment GLUT5 relative abundance did not differ significantly between whole-tissue homogenates (Table 1, Table 3, Fig. 5A).

Within PM fractions, GLUT5 did not show any significant effect with tissue, treatment, or their interaction. No significant effect was observed in the PM fraction of any tissue with fasting treatment (Table 2, Fig. 5B). Regardless of treatment, no significant difference was observed in the relative PM GLUT5 abundance among tissues (Table 4).

Discussion

Following a 1-hour treatment period, hummingbirds that were fasted ($n = 5$) had significantly lower blood fructose concentration (~ 0 mM) compared to those that continued to feed (~ 5 mM) ($n = 6$) (Figure 1). As this is the first report of blood fructose concentrations in hummingbirds, it is useful to compare our results against available data from other vertebrates that specialise on sugar-rich food sources. In frugivorous bats, such as the Egyptian fruit bat (*Rousettus aegyptiacus*), blood fructose concentrations rapidly rose from near-zero to ~ 11 mM following a fructose-only meal (Keegan, 1977). Blood fructose concentration of rats from the same study, representing non-sugar specialists, rose from zero to only ~ 0.5 mM, taking approximately 6 times longer than the bats to reach this peak (Keegan, 1977). Egyptian fruit bats, much like hummingbirds, have also been shown to rapidly incorporate fructose into their pool of metabolizable substrates (Keegan, 1977). Similarly, in the nectarivorous Pallas's long-tongued bat (*Glossophaga soricina*), the fraction of expired CO₂ supported by labelled carbons (f_{exo}) from

a fructose meal takes ~9 minutes to reach 50% (Voigt and Speakman, 2007) while it took ruby-throated hummingbirds ~14 minutes (Chen and Welch, 2014). In this study, we also observe relatively high blood fructose concentrations in fed hummingbirds followed by presumably rapid depletion to near-zero within an hour of fasting (Figure 1). We further observed a slightly higher lactate concentration in fasted hummingbirds, although not significantly so (Figure 1), suggesting elevated fructolytic pathway activity (Dekker et al., 2010). These results indicate a rapid depletion of circulating fructose levels and may imply the rapid incorporation of recently ingested fructose into the pool of metabolizable substrates in hummingbirds entering a fast.

In contrast, circulating concentrations of glucose were, as expected, high in fed hummingbirds (30.04 ± 2.03 mM). However, they remained elevated in fasted hummingbirds (29.67 ± 1.25 mM). This is slightly different from our predictions based on previous measurements Beuchat and Chong (1998) who observed a range of lower blood glucose concentrations (19-29 mM) in Anna's (*Calypte anna*) and Costa's hummingbirds (*Calypte costae*) after 1 hour of fasting. This discrepancy may partially be explained by differences in ingestion rates of sugars. McWhorter and Martínez del Río (2000) demonstrated that sugar ingestion rate in broad-tailed hummingbirds (*Selasphorus platycercus*) is negatively correlated with the concentration of sugar found in a meal. While Beuchat and Chong (1998) provided their hummingbirds with ~25% sucrose solution, ours was closer to ~33% sucrose. Furthermore, Beuchat et al. (1979) have shown variation in intestinal sugar uptake that are related to different energy management strategies employed by specific hummingbird species (as well as other nectarivores). Thus, it is possible that the relatively smaller ruby-throated hummingbird used in this study (~20% smaller than Anna's and Costa's hummingbirds), along with a slightly higher sugar concentration provided, resulted in a slightly extended duration of elevated blood glucose concentrations.

The relatively rapid depletion of circulating fructose compared to circulating glucose in ruby-throated hummingbirds is noteworthy. While hummingbirds are capable of directly metabolising fructose alone to power hovering flight (Chen and Welch, 2014), it may be that fructose is utilised first in order to reserve glucose for specific metabolic needs when both are present. Organs such as the brain are exceptionally demanding of glucose in *Gallus gallus* chicks (Tokushima et al., 2005), and likely in other birds as well. This demand may be exacerbated in

hummingbirds as their brain size is 2.5 times larger (relative to body weight) compared to galliform birds (Rehkämper et al., 1991). Lipogenic pathways of the hummingbird liver also show a preference for glucose over fructose (Dick et al., 2019). Finally, hummingbird flight muscle myofibrils' maximal capacity for monosaccharide phosphorylation is twice as high for glucose compared to fructose in tissue homogenates *in vitro* (Myrka and Welch, 2018). As the hummingbirds used in this study were perched in small jars that limited their movement, it may be that the initial fructose utilisation is sufficient for the maintenance of perching metabolism while glucose is reserved for greater or more specific energetic demands. This suggests that glucose uptake capacity is initially downregulated in hummingbirds entering a fast while fructose uptake capacity is unchanged. Alternatively, hummingbird blood fructose may undergo extensive and rapid conversion to glucose. As their muscles lack extensive glycogen stores (Suarez et al., 1990), processes such as gluconeogenesis from fructose in the liver or other tissues may underlie the maintenance of elevated blood glucose.

Control of glucose and fructose flux is well-described in avian species. Despite the absence of the insulin-GLUT4 system in avian muscle cells (Dupont, 2009), chickens and English sparrows (*Passer domesticus*) have demonstrated coordinated expression of GLUT isoforms to control sugar transmembrane transport (Sweazea and Braun, 2006; Wagstaff and White, 1995). Hummingbird GLUT expression and regulation is, however, relatively understudied, especially as access to tissue is limited and sample sizes remain relatively small including in this study. Here, using custom antibodies, we detected a strong immunoblot signal of the protein presence of GLUT 2, 3 and 5 in hummingbird flight muscle, heart, and liver tissue in whole-tissue homogenates (Table 1). GLUT2 was observed as a doublet while GLUT3 was detected at a size slightly larger than predicted, both of which may be attributable to variations in glycosylation (Asano et al., 1992; Ohtsubo et al., 2013). GLUT1 protein was detected in hummingbird flight muscle and heart (Table S1). GLUT1 protein in liver whole-tissue homogenates of ruby-throated hummingbirds was only minimally visible (Table 1) and was, surprisingly, not detected in PM fractions (Table 2). This result is in contrast to previously reported detection of hepatic mRNA transcript for GLUT1 in both chickens (Byers et al., 2018) and hummingbirds (Welch et al., 2013). However, as GLUT1 is abundant in erythrocytes (Carruthers, 2009), it is possible that the previous mRNA detection, as well as our detection of some hepatic GLUT1 protein, may have resulted from red blood cell contamination. While the presence of transcript does not necessarily

mean that the final protein form is being fully translated (Vogel and Marcotte, 2012), it is clear that hepatic GLUT1 is not translocated to the plasma membrane. Our findings are similar to others that have failed to detect GLUT1 in the avian liver (Byers et al., 2017; Carver et al., 2001), raising the possibility that the role of hepatic GLUT1 protein may be much more reduced among birds than previously appreciated.

In chickens, GLUT protein expression appears to be dependent on synthesis or degradation of protein (Yamada et al., 1983) rather than the translocation from cytosolic pools that is observed in mammalian cells (Guma et al., 1995). If the same were true in hummingbirds, GLUT abundance of the overall tissue should be tied to the abundance of GLUT protein in the PM. In this study, we noted that flight muscle whole-tissue homogenates showed the greatest response to fasting, in terms of relative GLUT abundance. We detected significantly lower GLUT1, GLUT2, and GLUT3 in flight muscle whole-tissue homogenates of fasted hummingbirds. While GLUTs only contribute to transmembrane transport of sugars when they are expressed in the PM, this reduction of glucose-specific GLUTs across the whole flight muscle tissue may underlie the reduced glucose uptake capacity. This may be especially important in their flight muscle as its metabolic demands overshadow that of other tissues during hovering (Suarez, 1992). Heart tissue of fasted hummingbirds showed no differences in GLUT abundance compared to fed hummingbirds in both whole-tissue and PM fraction samples. This muted response to fasting was expected as cardiac metabolism relies predominantly on circulating triglycerides (Pascual and Coleman, 2016). This may be especially true of hummingbirds as they routinely switch to fatty acid metabolism during periods of fasting (Welch et al., 2018). Alternatively, it may also imply that the elevated blood glucose concentration in hummingbirds entering a fast provides sufficient substrate for cardiac metabolism, especially given hummingbirds used in this study were constrained to continuously perch during the fasting period. Finally, in both liver whole-tissue homogenates and PM fractions, only GLUT3 was significantly lower in fasted hummingbirds. Chickens have also been shown to decrease their hepatic rate of glucose metabolism when fasted (Goodridge, 1968). And considering that we did not detect GLUT1 protein in liver PM fractions, this reduction in GLUT3 abundance during a fast in the liver might have a large effect on glucose import capacity.

Regardless of the total GLUT abundance of a given tissue, the functional capacity for sugar import into an active cell is dependent on the density of active GLUTs expressed in the PM (Wasserman, 2009). In this study, we detected significantly less GLUT1 protein in the flight muscle PM fractions and GLUT3 protein in liver PM fractions of fasted hummingbirds. This study is the first to report differences in subcellular abundance of GLUT protein in fed and fasted hummingbirds. Our results suggest that within the first hour of a fast, hummingbirds maintain elevated blood glucose levels through the lowering of glucose-specific glucose transporter abundance in the PM of these tissues. In this case, reduced expression of two high-affinity glucose-specific GLUTs in the PM, GLUT1 ($K_m \approx 3\text{-}5\text{mM}$; Zhao & Keating, 2007) and GLUT3 ($K_m \approx 1.5\text{mM}$; Mueckler & Thorens, 2013), may substantially impact the import of glucose into flight muscle and liver tissues, respectively. As we observed concordant decreases in GLUT1 in flight muscle and GLUT3 in liver whole-tissue homogenates, our data suggests that hummingbirds, much like chickens, regulate PM GLUT expression via synthesis or degradation of protein, rather than its translocation alone. Recently, a study measuring levels of chicken GLUT1 mRNA also noticed a decrease in transcript following fasting (Coudert et al., 2018). We further observed that the fructose-transporting GLUT2 (Fig. 3B) and GLUT5 (Fig. 5B), did not change in PM abundance in any tissues tested following the 1-hour fast (Table 2). GLUT5 abundance did not change in whole-tissue homogenates either for any tissues. This suggests that GLUT5 and GLUT2 remain constitutively expressed in the PM of hummingbirds entering a fast. As expression of PM GLUTs allows for rapid sugar import (Wasserman, 2009), and as the highest affinity for fructose that is exhibited by GLUT5 ($K_m \approx 11\text{-}12\text{mM}$; Douard & Ferraris, 2008), this constitutive PM GLUT expression may underlie the observed reduced blood fructose concentration in fasted hummingbirds.

In conclusion, we detected GLUTs 1, 2, 3, and 5 in all tissues, with the exception of GLUT1 in the liver PM. Flight muscle was observed to respond most dynamically to a 1-hour fast, followed by the liver, and finally the heart. We observed a decrease in the abundance of glucose-specific GLUT1 in flight muscle and GLUT3 in the liver in both whole-tissue homogenates and PM fractions. This may lead to reduced glucose import capacity and thus maintenance of elevated blood glucose concentrations in fasted hummingbirds. In addition, we observed the constitutive expression of fructose-transporting PM GLUT2 and PM GLUT5 in all tissues, which should permit continued fructose uptake into these tissues during initial stages of fasting, leading to near-depletion of the circulating pool of fructose. We further observed that the changes in GLUT protein expression occur both intracellularly and in the PM – no decrease of GLUT protein in the PM occurred without a concordant decrease in whole-tissue homogenates. These results suggest that hummingbirds, similar to other birds, may rely on mechanisms of GLUT synthesis and degradation, rather than translocation alone, to regulate extreme fluxes in circulating glucose and fructose concentrations.

Acknowledgements

We would like to thank Alex Myrka for his lessons on Western blotting and his advice during the entirety of the project. We are also grateful to the Welch Lab volunteers for their assistance with hummingbird capture. We extend a special thanks to Rachael Sparklin and Dr. Winston Timp for assembling the hummingbird transcriptome. Finally, we would like to thank Dr. Aarthi Ashok, Dr. Mauricio Terebiznik, and the Welch Lab team for their insights, critiques, and support.

Conflicting Interests

None to declare.

Funding

This research was supported by grants from the Natural Sciences and Engineering Research Council of Canada Discovery Grant (number 386466) to KCW and the Human Frontier Science Program (number RGP0062/2016) to KCW and GWW.

References

- Asano, T., Katagiri, H., Takata, K., Tsukuda, K., Lin, J.L., Ishihara, H., Inukai, K., Hirano, H., Yazaki, Y., Oka, Y., 1992. Characterization of GLUT3 protein expressed in Chinese hamster ovary cells. *Biochemical Journal* 288, 189–193.
<https://doi.org/10.1042/bj2880189>
- Bates, D., Mächler, M., Bolker, B., Walker, S., 2015. Fitting Linear Mixed-Effects Models Using lme4. *Journal of Statistical Software* 67. <https://doi.org/10.18637/jss.v067.i01>
- Beuchat, C.A., Chaplin, S.B., Morton, M.L., 1979. Ambient Temperature and the Daily Energetics of Two Species of Hummingbirds, *Calypte anna* and *Selasphorus rufus*. *Physiological Zoology* 52, 280–295. <https://doi.org/10.1086/physzool.52.3.30155751>
- Beuchat, C.A., Chong, C.R., 1998. Hyperglycemia in hummingbirds and its consequences for hemoglobin glycation. *Comparative Biochemistry and Physiology Part A: Molecular & Integrative Physiology* 120, 409–416.
- Boratyn, G.M., Schäffer, A.A., Agarwala, R., Altschul, S.F., Lipman, D.J., Madden, T.L., 2012. Domain enhanced lookup time accelerated BLAST. *Biology Direct* 7, 12.
<https://doi.org/10.1186/1745-6150-7-12>
- Byers, M.S., Bohannon-Stewart, A., Khwatenge, C., Alquireish, E., Alhathlol, A., Nahashon, S., Wang, X., 2018. Absolute Quantification of Tissue Specific Expression of Glucose Transporters in Chickens 1, 8.
- Byers, M.S., Howard, C., Wang, X., 2017. Avian and Mammalian Facilitative Glucose Transporters. *Microarrays* 6, 7. <https://doi.org/10.3390/microarrays6020007>
- Carruthers, A., 2009. Will the original glucose transporter isoform please stand up! *American Journal of Physiology-Endocrinology and Metabolism* 297, E836–E848.
<https://doi.org/10.1152/ajpendo.00496.2009>
- Carver, F.M., Shibley, Jr, I.A., Pennington, J.S., Pennington, S.N., 2001. Differential expression of glucose transporters during chick embryogenesis: *Cellular and Molecular Life Sciences* 58, 645–652. <https://doi.org/10.1007/PL00000887>
- Chen, C.C.W., Welch, K.C., 2014. Hummingbirds can fuel expensive hovering flight completely with either exogenous glucose or fructose. *Functional Ecology* 28, 589–600.
<https://doi.org/10.1111/1365-2435.12202>

- Chen, K.K., 1945. Susceptibility of birds to insulin as compared with mammals. *Journal of Pharmacology and Experimental Therapeutics* 84, 74–77.
- Coudert, E., Praud, C., Dupont, J., Crochet, S., Cailleau-Audouin, E., Bordeau, T., Godet, E., Collin, A., Berri, C., Tesseraud, S., Métayer-Coustard, S., 2018. Expression of glucose transporters SLC2A1, SLC2A8, and SLC2A12 in different chicken muscles during ontogenesis. *Journal of Animal Science* 96, 498–509. <https://doi.org/10.1093/jas/skx084>
- Dekker, M.J., Su, Q., Baker, C., Rutledge, A.C., Adeli, K., 2010. Fructose: a highly lipogenic nutrient implicated in insulin resistance, hepatic steatosis, and the metabolic syndrome. *American Journal of Physiology-Endocrinology and Metabolism* 299, E685–E694. <https://doi.org/10.1152/ajpendo.00283.2010>
- del Rio, M., Baker, H.G., Baker, I., 1992. Ecological and evolutionary implications of digestive processes: Bird preferences and the sugar constituents of floral nectar and fruit pulp. *Experientia* 48, 544–551. <https://doi.org/10.1007/BF01920237>
- Dick, M.F., Alcantara-Tangonan, A., Shamli Oghli, Y., Welch, K.C., 2019. Metabolic partitioning of sucrose and seasonal changes in fat turnover rate in ruby-throated hummingbirds (*Archilochus colubris*). *J Exp Biol jeb.212696*. <https://doi.org/10.1242/jeb.212696>
- Douard, V., Ferraris, R.P., 2008. Regulation of the fructose transporter GLUT5 in health and disease. *American Journal of Physiology-Endocrinology and Metabolism* 295, E227–E237. <https://doi.org/10.1152/ajpendo.90245.2008>
- Dupont, J., 2009. Insulin signaling in chicken liver and muscle. *General and Comparative Endocrinology* 163, 52–57. <https://doi.org/10.1016/j.ygcen.2008.10.016>
- Eberts, E., Dick, M., Welch, K., 2019. Metabolic Fates of Evening Crop-Stored Sugar in Ruby-Throated Hummingbirds (*Archilochus colubris*). *Diversity* 11, 9. <https://doi.org/10.3390/d11010009>
- Egert, S., Nguyen, N., Schwaiger, M., 1999. Myocardial Glucose Transporter GLUT1: Translocation Induced by Insulin and Ischemia. *Journal of Molecular and Cellular Cardiology* 31, 1337–1344. <https://doi.org/10.1006/jmcc.1999.0965>
- Gassmann, M., Grenacher, B., Rohde, B., Vogel, J., 2009. Quantifying Western blots: Pitfalls of densitometry. *ELECTROPHORESIS* 30, 1845–1855. <https://doi.org/10.1002/elps.200800720>

- Gasteiger, E., Hoogland, C., Gattiker, A., Duvaud, S., Wilkins, M.R., Appel, R.D., Bairoch, A., 2005. Protein Identification and Analysis Tools on the ExPASy Server, in: Walker, J.M. (Ed.), *The Proteomics Protocols Handbook*. Humana Press, Totowa, NJ, pp. 571–607. <https://doi.org/10.1385/1-59259-890-0:571>
- Godoy, A., Ulloa, V., Rodríguez, F., Reinicke, K., Yañez, A.J., García, M. de los A., Medina, R.A., Carrasco, M., Barberis, S., Castro, T., Martínez, F., Koch, X., Vera, J.C., Poblete, M.T., Figueroa, C.D., Peruzzo, B., Pérez, F., Nualart, F., 2006. Differential subcellular distribution of glucose transporters GLUT1–6 and GLUT9 in human cancer: Ultrastructural localization of GLUT1 and GLUT5 in breast tumor tissues. *J. Cell. Physiol.* 207, 614–627. <https://doi.org/10.1002/jcp.20606>
- Guma, A., Zierath, J.R., Wallberg-Henriksson, H., Klip, A., 1995. Insulin induces translocation of GLUT-4 glucose transporters in human skeletal muscle. *American Journal of Physiology-Endocrinology and Metabolism* 268, E613–E622. <https://doi.org/10.1152/ajpendo.1995.268.4.E613>
- Han, J., Gagnon, S., Eckle, T., Borchers, C.H., 2013. Metabolomic analysis of key central carbon metabolism carboxylic acids as their 3-nitrophenylhydrazones by UPLC/ESI-MS: General. *ELECTROPHORESIS* n/a-n/a. <https://doi.org/10.1002/elps.201200601>
- Han, J., Lin, K., Sequira, C., Yang, J., Borchers, C.H., 2016. Quantitation of low molecular weight sugars by chemical derivatization-liquid chromatography/multiple reaction monitoring/mass spectrometry: Liquid Phase Separations. *ELECTROPHORESIS* 37, 1851–1860. <https://doi.org/10.1002/elps.201600150>
- Hussar, P., Järveots, T., Dūrītis, I., 2019. Immunolocalization of hexose transporters in ostriches' intestinal epithelial cells during their first postnatal week. *PoA* 28, 61–67. <https://doi.org/10.12697/poa.2019.28.1.05>
- Karasov, W.H., 2017. Integrative physiology of transcellular and paracellular intestinal absorption. *The Journal of Experimental Biology* 220, 2495–2501. <https://doi.org/10.1242/jeb.144048>
- Keegan, D.J., 1977. Aspects of the assimilation of sugars by *Rousettus aegyptiacus*. *Comparative Biochemistry and Physiology Part A: Physiology* 58, 349–352. [https://doi.org/10.1016/0300-9629\(77\)90153-0](https://doi.org/10.1016/0300-9629(77)90153-0)

- Klip, A., Volchuk, A., He, L., Tsakiridis, T., 1996. The glucose transporters of skeletal muscle. *Seminars in Cell & Developmental Biology* 7, 229–237.
<https://doi.org/10.1006/scdb.1996.0031>
- Lenth, R., 2019. emmeans: Estimated Marginal Means, aka Least-Squares Means. R package version 1.4.
- Mathieu-Costello, O., Suarez, R., Hochachka, P.W., 1992. Capillary-to-fiber geometry and mitochondrial density in hummingbird flight muscle. *Respiration physiology* 89, 113–132.
- McWhorter, T.J., Martínez del Rio, C., 2000. Does Gut Function Limit Hummingbird Food Intake? *Physiological and Biochemical Zoology* 73, 313–324.
<https://doi.org/10.1086/316753>
- Mueckler, M., Thorens, B., 2013. The SLC2 (GLUT) family of membrane transporters. *Molecular Aspects of Medicine* 34, 121–138. <https://doi.org/10.1016/j.mam.2012.07.001>
- Myrka, A.M., Welch, K.C., 2018. Evidence of high transport and phosphorylation capacity for both glucose and fructose in the ruby-throated hummingbird (*Archilochus colubris*). *Comparative Biochemistry and Physiology Part B: Biochemistry and Molecular Biology* 224, 253–261. <https://doi.org/10.1016/j.cbpb.2017.10.003>
- Ohtsubo, K., Takamatsu, S., Gao, C., Korekane, H., Kurosawa, T.M., Taniguchi, N., 2013. N-glycosylation modulates the membrane sub-domain distribution and activity of glucose transporter 2 in pancreatic beta cells. *Biochemical and Biophysical Research Communications* 434, 346–351. <https://doi.org/10.1016/j.bbrc.2013.03.076>
- Pascual, F., Coleman, R.A., 2016. Fuel availability and fate in cardiac metabolism: A tale of two substrates. *Biochimica et Biophysica Acta (BBA) - Molecular and Cell Biology of Lipids* 1861, 1425–1433. <https://doi.org/10.1016/j.bbalip.2016.03.014>
- Price, E.R., Brun, A., Caviedes-Vidal, E., Karasov, W.H., 2015. Digestive Adaptations of Aerial Lifestyles. *Physiology* 30, 69–78. <https://doi.org/10.1152/physiol.00020.2014>
- Rehkämper, G., Schuchmann, K.-L., Schleicher, A., Zilles, K., 1991. Encephalization in Hummingbirds (Trochilidae). *Brain Behav Evol* 37, 85–91.
<https://doi.org/10.1159/000114349>

- Rodriguez-Peña, N., Price, E.R., Caviedes-Vidal, E., Flores-Ortiz, C.M., Karasov, W.H., 2016. Intestinal paracellular absorption is necessary to support the sugar oxidation cascade in nectarivorous bats. *J Exp Biol* 219, 779–782. <https://doi.org/10.1242/jeb.133462>
- Simon, J., Rideau, N., Taouis, M., Dupont, J., 2011. Plasma insulin levels are rather similar in chicken and rat. *General and Comparative Endocrinology* 171, 267–268. <https://doi.org/10.1016/j.ygcen.2011.02.025>
- Simpson, I.A., Dwyer, D., Malide, D., Moley, K.H., Travis, A., Vannucci, S.J., 2008. The facilitative glucose transporter GLUT3: 20 years of distinction. *American Journal of Physiology-Endocrinology and Metabolism* 295, E242–E253. <https://doi.org/10.1152/ajpendo.90388.2008>
- Steane, S.E., Mylott, D., White, M.K., 1998. Regulation of a Heterologous Glucose Transporter Promoter in Chicken Embryo Fibroblasts. *Biochemical and Biophysical Research Communications* 252, 318–323. <https://doi.org/10.1006/bbrc.1998.9616>
- Suarez, R., 1992. Hummingbird flight: Sustaining the highest mass-specific metabolic rates among vertebrates. *Experientia* 48, 565–570. <https://doi.org/10.1007/BF01920240>
- Suarez, R., Brownsey, R.W., Vogl, W., Brown, G.S., Hochachka, P.W., 1988. Biosynthetic capacity of hummingbird liver. *American Journal of Physiology-Regulatory, Integrative and Comparative Physiology* 255, R699–R702. <https://doi.org/10.1152/ajpregu.1988.255.5.R699>
- Suarez, R., Lighton, J.R., Moyes, C.D., Brown, G.S., Gass, C.L., Hochachka, P.W., 1990. Fuel selection in rufous hummingbirds: ecological implications of metabolic biochemistry. *Proceedings of the National Academy of Sciences* 87, 9207–9210. <https://doi.org/10.1073/pnas.87.23.9207>
- Suarez, R., Welch, K., 2017. Sugar Metabolism in Hummingbirds and Nectar Bats. *Nutrients* 9, 743. <https://doi.org/10.3390/nu9070743>
- Suarez, R., Welch, K.C., 2011. The sugar oxidation cascade: aerial refueling in hummingbirds and nectar bats. *Journal of Experimental Biology* 214, 172–178. <https://doi.org/10.1242/jeb.047936>
- Sweazea, K.L., Braun, E.J., 2006. Glucose transporter expression in English sparrows (*Passer domesticus*). *Comparative Biochemistry and Physiology Part B: Biochemistry and Molecular Biology* 144, 263–270. <https://doi.org/10.1016/j.cbpb.2005.12.027>

- Thorens, Mueckler, M., 2010. Glucose transporters in the 21st Century. *American Journal of Physiology-Endocrinology and Metabolism* 298, E141–E145.
<https://doi.org/10.1152/ajpendo.00712.2009>
- Tokushima, Y., Takahashi, K., Sato, K., Akiba, Y., 2005. Glucose uptake in vivo in skeletal muscles of insulin-injected chicks. *Comparative Biochemistry and Physiology Part B: Biochemistry and Molecular Biology* 141, 43–48.
<https://doi.org/10.1016/j.cbpc.2005.01.008>
- Vogel, C., Marcotte, E.M., 2012. Insights into the regulation of protein abundance from proteomic and transcriptomic analyses. *Nature Reviews Genetics* 13, 227–232.
<https://doi.org/10.1038/nrg3185>
- Voigt, C.C., Speakman, J.R., 2007. Nectar-feeding bats fuel their high metabolism directly with exogenous carbohydrates. *Funct Ecology* 21, 913–921. <https://doi.org/10.1111/j.1365-2435.2007.01321.x>
- Wagstaff, P., White, M.K., 1995. Characterization of the Avian GLUT1 Glucose Transporter: Differential Regulation of GLUT1 and GLUT3 in Chicken Embryo Fibroblasts. *Molecular Biology of the Cell* 6, 15.
- Wasserman, D.H., 2009. Four grams of glucose. *American Journal of Physiology-Endocrinology and Metabolism* 296, E11–E21. <https://doi.org/10.1152/ajpendo.90563.2008>
- Wasserman, D.H., Kang, L., Ayala, J.E., Fueger, P.T., Lee-Young, R.S., 2011. The physiological regulation of glucose flux into muscle in vivo. *Journal of Experimental Biology* 214, 254–262. <https://doi.org/10.1242/jeb.048041>
- Welch, K.C., Allalou, A., Sehgal, P., Cheng, J., Ashok, A., 2013. Glucose Transporter Expression in an Avian Nectarivore: The Ruby-Throated Hummingbird (*Archilochus colubris*). *PLoS ONE* 8, e77003. <https://doi.org/10.1371/journal.pone.0077003>
- Welch, K.C., Myrka, A.M., Ali, R.S., Dick, M.F., 2018. The Metabolic Flexibility of Hovering Vertebrate Nectarivores. *Physiology* 33, 127–137.
<https://doi.org/10.1152/physiol.00001.2018>
- Wood, I.S., Trayhurn, P., 2003. Glucose transporters (GLUT and SGLT): expanded families of sugar transport proteins. *British Journal of Nutrition* 89, 3.
<https://doi.org/10.1079/BJN2002763>

- Workman, R.E., Myrka, A.M., Wong, G.W., Tseng, E., Welch, K.C., Timp, W., 2018. Single-molecule, full-length transcript sequencing provides insight into the extreme metabolism of the ruby-throated hummingbird *Archilochus colubris*. *GigaScience* 7.
<https://doi.org/10.1093/gigascience/giy009>
- Yamada, K., Tillotson, L.G., Isselbacher, K.J., 1983. Regulation of Hexose Carriers in Chicken Embryo Fibroblasts. *The Journal of Biological Chemistry* 258, 9786–9792.
- Yamamoto, N., Yamashita, Y., Yoshioka, Y., Nishiumi, S., Ashida, H., 2016. Rapid Preparation of a Plasma Membrane Fraction: Western Blot Detection of Translocated Glucose Transporter 4 from Plasma Membrane of Muscle and Adipose Cells and Tissues. *Curr Protoc Protein Sci.* 85:29, 1–29.
- Yang, J., Holman, G., D., 1993. Comparison of GLUT4 and GLUT 1 Subcellular Trafficking in Basal and Insulin-stimulated 3T3-L1 Cells. *The Journal of Biological Chemistry* 268, 4600–4603.
- Zhang, W., Sumners, L.H., Siegel, P.B., Cline, M.A., Gilbert, E.R., 2013. Quantity of glucose transporter and appetite-associated factor mRNA in various tissues after insulin injection in chickens selected for low or high body weight. *Physiological Genomics* 45, 1084–1094. <https://doi.org/10.1152/physiolgenomics.00102.2013>
- Zhao, F.Q., Glimm, D.R., Kennelly, J.J., 1993. Distribution of mammalian facilitative glucose transporter messenger RNA in bovine tissues. *International Journal of Biochemistry* 25, 1897–1903. [https://doi.org/10.1016/0020-711X\(88\)90322-9](https://doi.org/10.1016/0020-711X(88)90322-9)
- Zhao, F.Q., Keating, A.F., 2007. Functional Properties and Genomics of Glucose Transporters. *Current Genomics* 8, 113–128.

Tables and Figures

Table 1: Relative whole-tissue abundance of GLUT1, GLUT2, GLUT3, and GLUT5 in flight muscle, heart, and liver of fed and fasted hummingbirds. Data and representative immunoblots are presented here for the whole tissue homogenates of hummingbird tissue. Fasted/fed ratios reflect the relative variation in GLUT protein abundance with fasting treatment. Observed molecular weights (M.W.) are reported. Sample sizes are given for the number of 1) fed hummingbirds, 2) fasted hummingbirds. Asterisks (*) indicate $p < 0.05$.


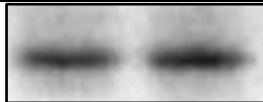

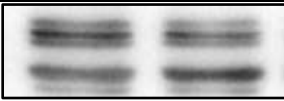

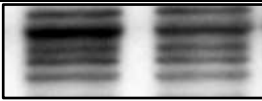

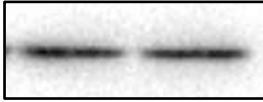
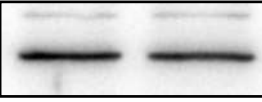
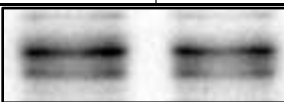

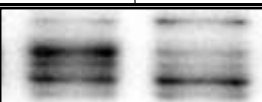
Whole Tissue Homogenate	M.W. (kDa)	Flight Muscle		Heart		Liver	
		Fed	Fast	Fed	Fast	Fed	Fast
GLUT1	47.0 →						
		Fasted/Fed Ratio		Fasted/Fed Ratio		Fasted/Fed Ratio	
		0.73 ± 0.09		0.81 ± 0.16		0.60 ± 0.10	
		$p = 0.010^*$	$n = 6, 6$	$p = 0.370$	$n = 2, 2$	$p = 0.126$	$n = 3, 3$
GLUT2	43.5 →						
		Fasted/Fed Ratio		Fasted/Fed Ratio		Fasted/Fed Ratio	
		0.54 ± 0.08		0.75 ± 0.16		0.96 ± 0.17	
		$p = 0.019^*$	$n = 4, 4$	$p = 0.134$	$n = 2, 2$	$p = 0.786$	$n = 3, 3$
GLUT3	72.4 →						
		Fasted/Fed Ratio		Fasted/Fed Ratio		Fasted/Fed Ratio	
		0.68 ± 0.09		0.82 ± 0.16		0.58 ± 0.09	
		$p = 0.015^*$	$n = 4, 4$	$p = 0.626$	$n = 2, 2$	$p = 0.0001^*$	$n = 3, 3$
GLUT5	55.3 →						
		Fasted/Fed Ratio		Fasted/Fed Ratio		Fasted/Fed Ratio	
		1.11 ± 0.27		0.82 ± 0.36		1.28 ± 0.36	
		$p = 0.350$	$n = 4, 4$	$p = 0.987$	$n = 2, 2$	$p = 0.554$	$n = 3, 3$

Table 2: Relative PM abundance of GLUT1, GLUT2, GLUT3, and GLUT5 in flight muscle, heart, and liver of fed and fasted hummingbirds. Data and representative immunoblots are presented here for hummingbird tissue samples that underwent plasma membrane fractionation; only PM-residing GLUTs are presented. Fasted/fed ratios reflect the relative variation in GLUT protein abundance with fasting treatment. Observed molecular weights (M.W.) are reported. Sample sizes are given for the number of 1) fed hummingbirds, 2) fasted hummingbirds. Asterisks (*) indicate $p < 0.05$.



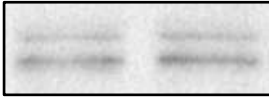




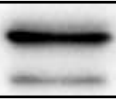

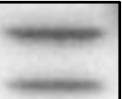

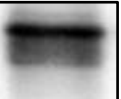


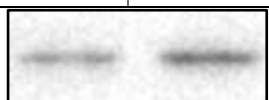

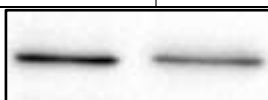







Plasma Membrane Fraction	M.W. (kDa)	Flight Muscle		Heart		Liver	
		Fed	Fast	Fed	Fast	Fed	Fast
GLUT1	47.0 →						
Fasted/Fed Ratio		0.61 ± 0.06		1.20 ± 0.15		N/A	
		$p = 0.002^*$	$n = 6, 6$	$p = 0.500$	$n = 4, 5$	N/A	N/A
GLUT2	43.5 →						
Fasted/Fed Ratio		0.81 ± 0.12		1.06 ± 0.14		0.96 ± 0.16	
		$p = 0.300$	$n = 4, 4$	$p = 0.584$	$n = 5, 5$	$p = 0.792$	$n = 3, 3$
GLUT3	72.4 →						
Fasted/Fed Ratio		0.90 ± 0.14		0.99 ± 0.14		0.58 ± 0.10	
		$p = 0.903$	$n = 4, 4$	$p = 1.000$	$n = 5, 5$	$p = 0.004^*$	$n = 3, 3$
GLUT5	55.3 →						
Fasted/Fed Ratio		0.17 ± 0.30		1.13 ± 0.26		0.89 ± 0.27	
		$p = 0.308$	$n = 4, 4$	$p = 0.864$	$n = 5, 5$	$p = 0.754$	$n = 3, 3$

Table 3: Relative abundance of GLUT1, GLUT2, GLUT3, and GLUT5 among whole-tissue homogenates compared pair-wise between flight muscle, heart, and liver of fed and fasted hummingbirds. Data represents the relative whole-tissue GLUT abundance. Asterisks (*) indicate $p < 0.05$.

Whole Tissue Homogenate	GLUT Isoform	Relative Fed Ratio	<i>p</i> -value	Tissue Sample Size	Relative Fasted Ratio	<i>p</i> -value	Tissue Sample Size
Flight Muscle / Heart	GLUT1	1.95 ± 0.54	0.082	6, 2	1.76 ± 0.49	0.120	6, 2
	GLUT2	0.70 ± 0.35	0.486	4, 2	0.37 ± 0.18	0.399	4, 2
	GLUT3	1.59 ± 0.31	0.175	4, 2	1.32 ± 0.26	0.712	4, 2
	GLUT5	1.82 ± 1.37	0.911	4, 2	2.45 ± 1.97	0.887	4, 2
Flight Muscle / Liver	GLUT1	4.75 ± 1.27	0.040*	6, 3	5.76 ± 1.54	0.046*	6, 3
	GLUT2	0.65 ± 0.32	0.386	4, 3	0.37 ± 0.12	0.068	4, 3
	GLUT3	0.65 ± 0.11	0.086	4, 3	0.75 ± 0.13	0.429	4, 3
	GLUT5	0.59 ± 0.53	0.985	4, 3	0.52 ± 0.46	0.816	4, 3
Heart / Liver	GLUT1	2.44 ± 0.83	0.147	2, 3	3.28 ± 1.11	0.075	2, 3
	GLUT2	0.93 ± 0.52	0.992	2, 3	0.73 ± 0.41	0.699	2, 3
	GLUT3	0.41 ± 0.08	0.014*	2, 3	0.57 ± 0.11	0.185	2, 3
	GLUT5	0.33 ± 0.29	0.697	2, 3	0.21 ± 0.20	0.350	2, 3

Table 4: Relative abundance of GLUT1, GLUT2, GLUT3, and GLUT5 among PM fractions of flight muscle, heart, and liver of fed and fasted hummingbirds. Values represent the relative abundance of GLUT proteins from isolated plasma membrane samples (fractionation efficiency approx. $92.1 \pm 0.5\%$; see Table S2). Asterisks (*) indicate $p < 0.05$.

Plasma Mem. Fraction	GLUT Isoform	Relative Fed Ratio	<i>p</i> -value	Tissue Sample Size	Relative Fasted Ratio	<i>p</i> -value	Tissue Sample Size
Flight Muscle / Heart	GLUT1	4.87 ± 1.30	0.009*	6, 4	2.48 ± 0.66	0.075	6, 5
	GLUT2	2.31 ± 2.20	0.782	4, 5	1.77 ± 1.67	0.835	4, 5
	GLUT3	1.68 ± 0.79	0.814	4, 5	1.53 ± 0.71	0.950	4, 5
	GLUT5	1.84 ± 1.18	0.451	4, 5	1.96 ± 1.24	0.318	4, 5
Flight Muscle / Liver	GLUT1	<i>Not detected in liver PM</i>			<i>Not detected in liver PM</i>		
	GLUT2	1.19 ± 1.37	0.954	4, 3	1.00 ± 1.16	0.980	4, 3
	GLUT3	0.48 ± 0.27	0.396	4, 3	0.74 ± 0.42	0.958	4, 3
	GLUT5	0.61 ± 0.47	0.976	4, 3	0.39 ± 0.30	0.747	4, 3
Heart / Liver	GLUT1	<i>Not detected in liver PM</i>			<i>Not detected in liver PM</i>		
	GLUT2	0.51 ± 0.59	0.961	5, 3	0.57 ± 0.65	0.954	5, 3
	GLUT3	0.28 ± 0.16	0.225	5, 3	0.48 ± 0.27	0.730	5, 3
	GLUT5	0.33 ± 0.25	0.643	5, 3	0.20 ± 0.15	0.747	5, 3

Figures

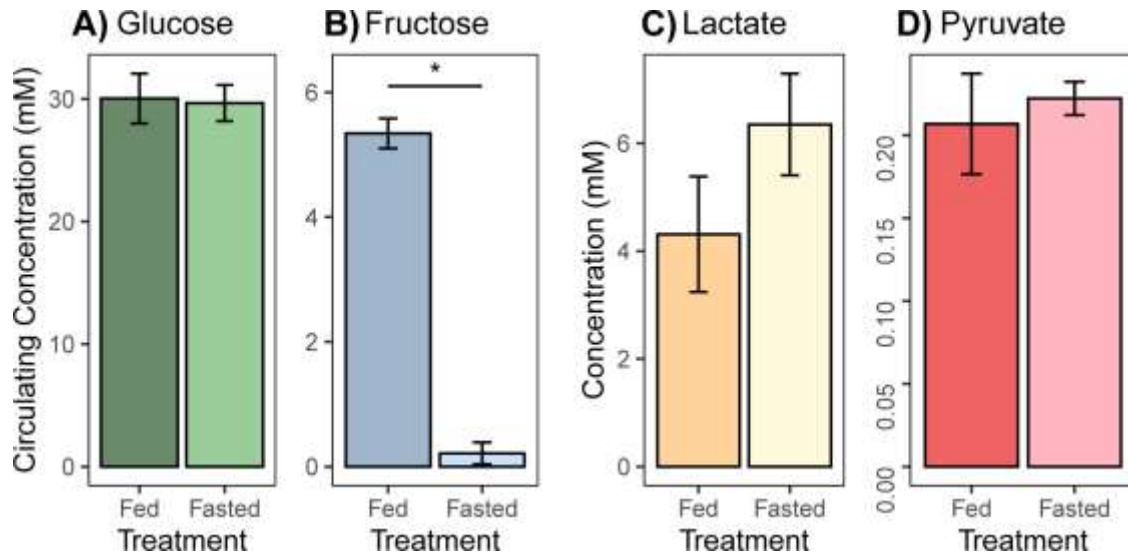


Figure 1: Mean concentrations (mM) \pm standard error of circulating sugars A) Glucose, B) Fructose from plasma samples and metabolites C) Lactate, D) Pyruvate from flight muscle homogenates of fed ($n = 6$) and fasted ($n = 5$) male hummingbirds. Data is presented as mean concentration in millimoles/litre \pm standard error (A, B) and millimoles/gram \pm standard error (C, D). Asterisk (*) indicates $p = 0.001$.

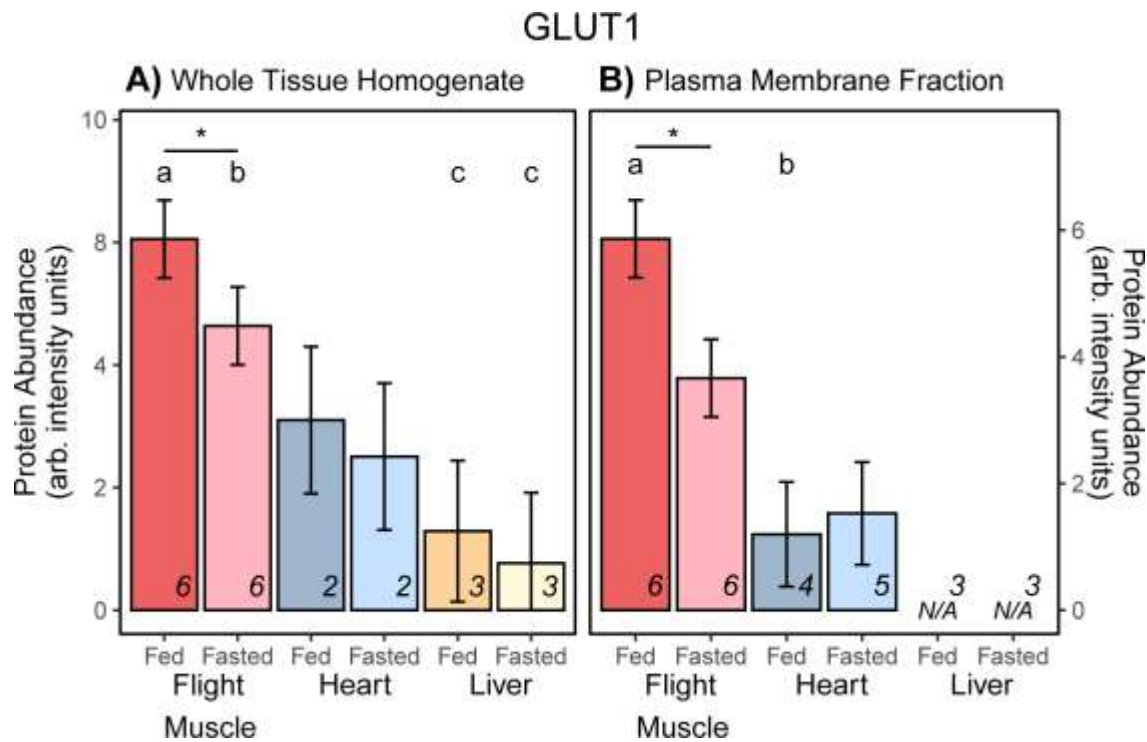


Figure 2. Relative protein abundance of GLUT1 in hummingbird flight muscle, heart, and liver tissue. Data represents mean \pm standard error of arbitrary units of intensity based on analyses of normalised immunoblots. *Ad-libitum* fed (“Fed”) and 1-hour fasted (“Fasted”) hummingbird GLUT1 abundance was measured in A) whole-tissue homogenates and B) plasma membrane fraction samples. An asterisk (*) over a tissue group indicates a significant difference ($p < 0.05$) of GLUT1 between fed and fasted conditions within that tissue, summarised in Table 1 and Table 2. Letters (a, b, c) over individual bars represent a significant difference ($p < 0.05$) of GLUT1 abundance between the specified tissue under the treatment condition, summarised in Table 3 and Table 4. Sample sizes are superimposed on the bottom-right for each tissue and treatment.

GLUT2

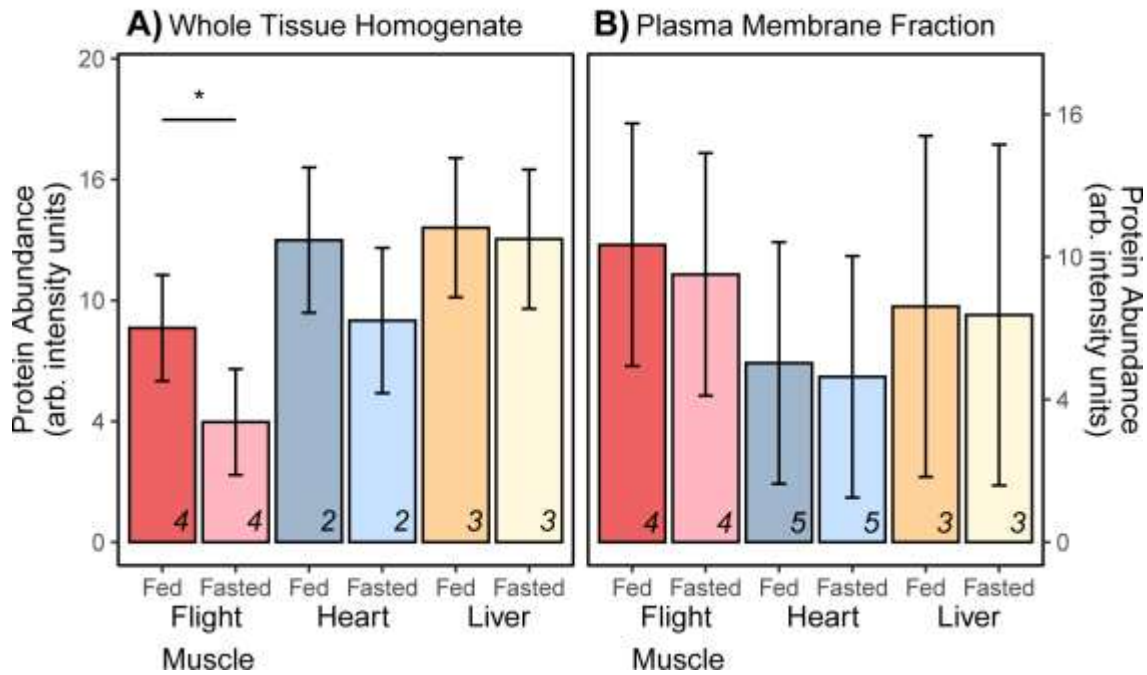


Figure 3. Relative protein abundance of GLUT2 in hummingbird flight muscle, heart, and liver tissue. Data represents mean \pm standard error of arbitrary units of intensity based on analyses of normalised immunoblots. *Ad-libitum* fed (“Fed”) and 1-hour fasted (“Fasted”) hummingbird GLUT2 abundance was measured in A) whole tissue homogenates and B) plasma membrane fraction samples. An asterisk (*) over a tissue group indicates a significant difference ($p < 0.05$) of GLUT2 between fed and fasted conditions within that tissue, summarised in Table 1 and Table 2. Differences in GLUT2 abundance between tissues within the treatment condition are summarised in Table 3 and Table 4. Sample sizes are superimposed on the bottom-right for each tissue and treatment.

GLUT3

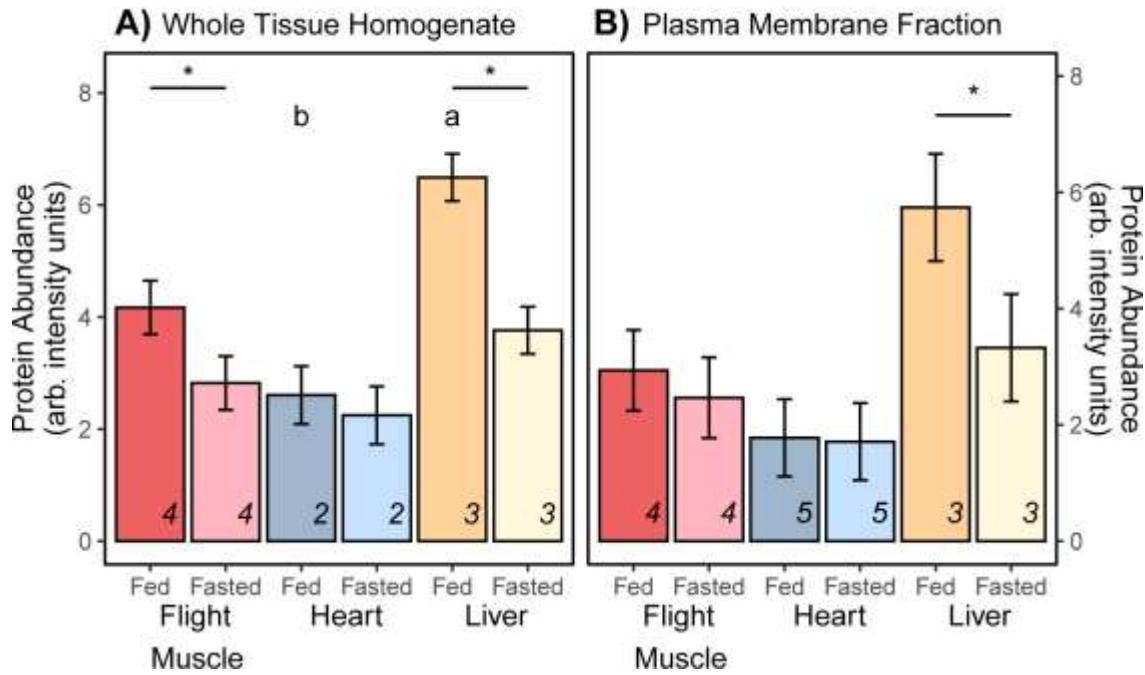


Figure 4. Relative protein abundance of GLUT3 in hummingbird flight muscle, heart, and liver tissue. Data represents mean \pm standard error of arbitrary units of intensity based on analyses of normalised immunoblots. *Ad-libitum* fed (“Fed”) and 1-hour fasted (“Fasted”) hummingbird GLUT3 abundance was measured in A) whole tissue homogenates and B) plasma membrane fraction samples. An asterisk (*) over a tissue group indicates a significant difference ($p < 0.05$) of GLUT3 between fed and fasted conditions within that tissue, summarised in Table 1 and Table 2. Letters (a, b) over individual bars represent a significant difference ($p < 0.05$) of GLUT3 abundance between the specified tissue under the treatment condition, summarised in Table 3 and Table 4. Sample sizes are superimposed on the bottom-right for each tissue and treatment.

GLUT5

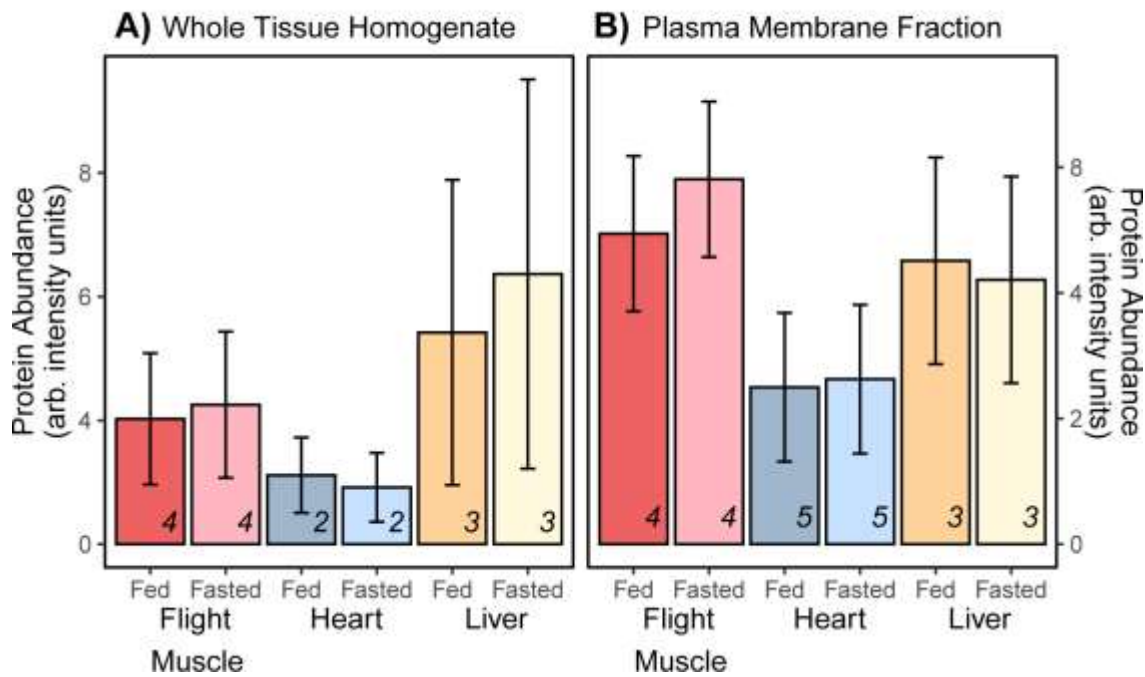


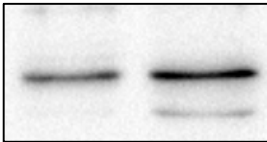
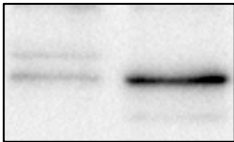
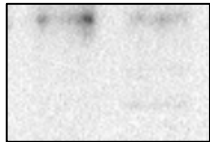
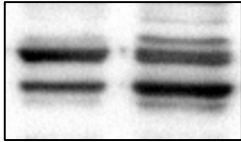
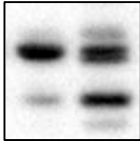
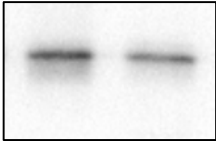
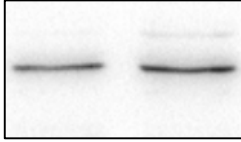
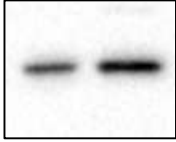
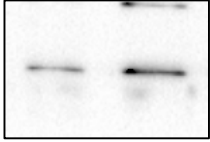
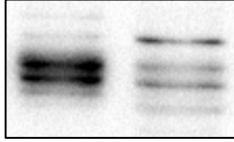
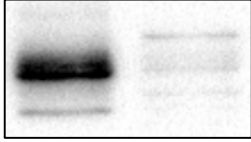
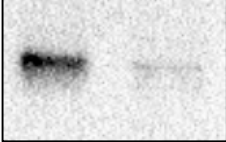
Figure 5. Relative protein abundance of GLUT5 in hummingbird flight muscle, heart, and liver tissue. Data represents mean \pm standard error of arbitrary units of intensity based on analyses of normalised immunoblots. *Ad-libitum* fed (“Fed”) and 1-hour fasted (“Fasted”) hummingbird GLUT5 abundance was measured in A) whole tissue homogenates and B) plasma membrane fraction samples. Differences in GLUT5 abundance between fed and fasted conditions within a given tissue are summarised in Table 1 and Table 2. Differences in GLUT5 abundance between tissues within the treatment condition are summarised in Table 3 and Table 4. Sample sizes are superimposed on the bottom-right for each tissue and treatment.

Supplementary Materials

3.1 Custom antibodies: GLUT1, 2, 3, and 5 detection in PM and WTH samples.

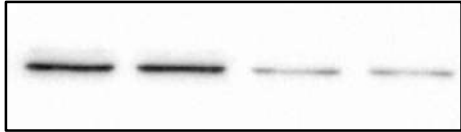
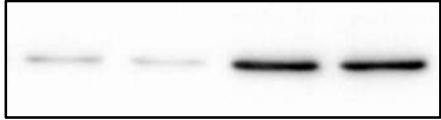
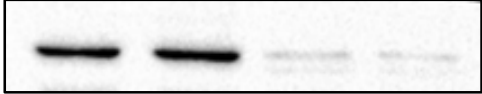
Table S1: GLUTs 1, 2, 3, and 5 observed molecular weights in plasma membrane (PM) fractions and whole-tissue homogenates (WTH) of flight muscle, heart, and liver.

Representative immunoblots are shown for each tissue and fraction.

Observed Molecular Weight	Flight Muscle		Heart		Liver	
	PMF	WTH	PMF	WTH	PMF	WTH
GLUT1 Predicted mW = 53.8 kDa	47.0 kDa →					
GLUT2 Predicted mW = 57.9 kDa	43.5 kDa →					
GLUT3 Predicted mW = 53.3 kDa	72.4 kDa →					
GLUT5 Predicted mW = 56.9 kDa	55.3 kDa →					

3.2 Plasma Membrane Fractionation Purity

Table S2: Relative distribution of known cytosolic or PM-residing proteins following PM fractionation. Fraction purity indicates the relative abundance of protein in either the PM-only fraction compared to the without-PM-fraction (i.e. cytosolic proteins only).

	Observed Molecular Weight	Plasma Membrane Fraction	Cytosolic Fraction (PM proteins removed)
E-Cadherin (PM-residing protein)	74.3kDa →		
	Fraction staining intensity:	92.1 ± 1.8 %	7.9 ± 1.8 %
GAPDH (cytosolic protein)	34.9 kDa →		
	Fraction staining intensity:	5.9 ± 0.5 %	94.1 ± 0.5 %
Na⁺/K⁺ ATPase (PM-residing protein)	103.1 kDa →		
	Fraction staining intensity:	92.1 ± 0.5 %	7.8 ± 0.5 %

3.3 GLUT Amino Acid Sequence and Antibody Epitope

Table S3: Immunoblots on lysates of overexpressed GLUT1, GLUT2, GLUT3, GLUT5 protein. Each immunoblot lane represents a cell lysate produced from an entire well of a 6-well cell-culture dish. Isoform specificity was tested via immunoblotting all cell lysates (empty vector control, acGLUT1, 2, 3, and 5) with each novel GLUT antibody and observing GLUT protein signal overlap. Anti-V5 tag represents targeted immunostaining of all GLUT protein expressed in that cell lysate. Black arrows refer to the band representing the GLUT protein isoform.

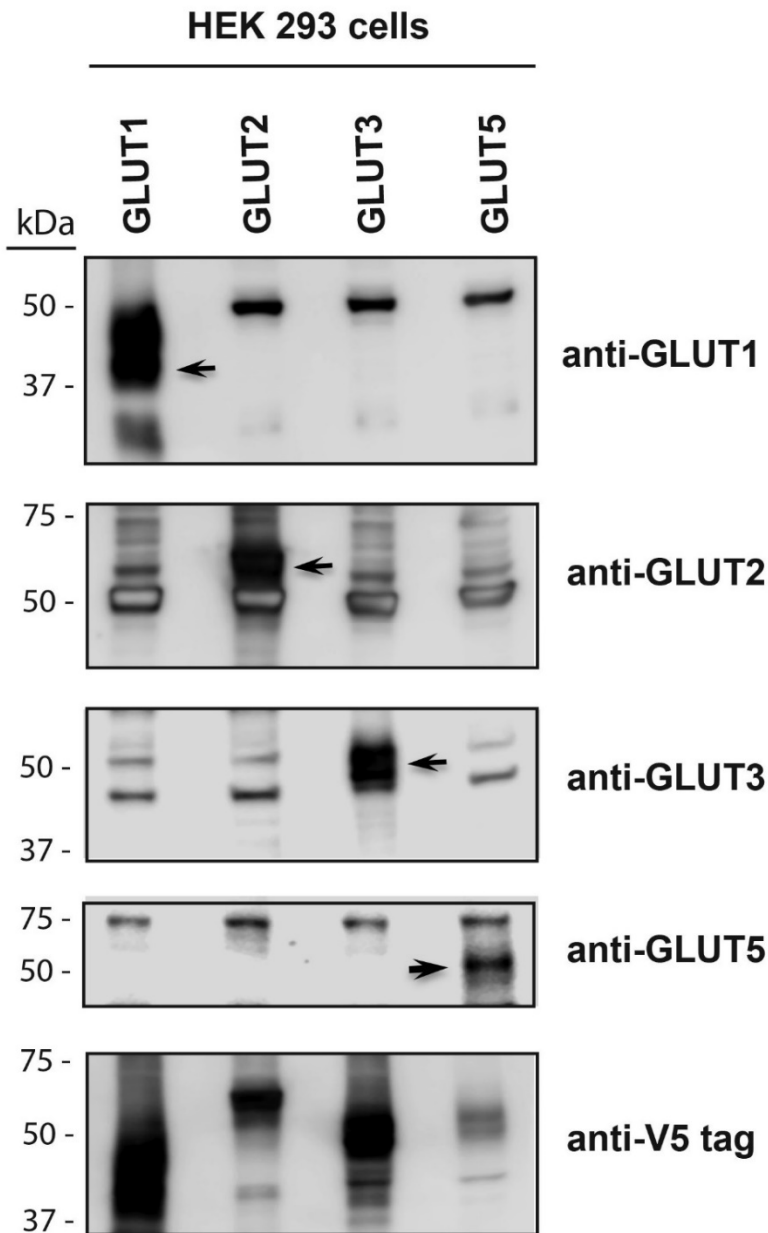


Table S4: Ruby-throated hummingbird specific GLUT1, GLUT2, GLUT3 and GLUT5 protein sequences. Highlighted regions indicated epitope targeted during antibody development to ensure greatest dissimilarity between targeted isoforms

Protein/Gene	Amino Acid Sequence
GLUT1/SLC2A1	METGSKMTARLMLAVGGAVLGS LQFGYNTGVINAPQKVIEDFYNRTWLRYE E PITSATLTT LWLSVAIFSVGGMVGSFSVGLFVNRFGRRRNSMLMSNILAFLAAVLMGFSKMALSFEMLL GRFIIGLYSGLTTGFVPMYVEVSPTALRGALGTFHQLGIVLGILVAQVFLGLDLMGNDLWLP LLLGFI FVPALLQCIILPFAPESPRFLLINRNEENKAKSVLKKLRGTTDVSDDLQEMKEESRQMM REKKVTIMELFRSPMYRQPILIAIVLQLSQQLSGINAVFYSTSI FEKSGVEQP VYATIGSGVNT AFTVVSLFVVERAGRRTLHLIGLAGMAGCAVLMTIALTLDDQMPWMSYLSIVAIFGFVAF FEI GPGPIWPFIVAELFSQGPRPAFAVAGLSNWTSNFIVGMGFQYIAQLCGSYVFIIFTVLLILFFI FTYFKVPETKGRTFDEIA SGFRQGGAGQSDKTPDEFHS LGADSQV <i>NCBI Accession Number: MT472837</i>
GLUT2/SLC2A2	MDKKNKMQA EKHLTGLVLSVFAAVLGFFQYGYSLGVINAPQKVIEAHYGRVLGIAPPDRFP TSASEEDGTVPVTEPWVSTEATLAPEDDPGEDLGTSSHILTMYSLSVSMFAVGGMVSSFT VGWIGDRLGRVKAMLV VNILSIIGNLLMGLAKFGPSHMLIIAGRAVTGLYCGLSSGLVPMYVS EVSPTALRGALGTLHQLAIVTGILISQVLGLDFLLGNDEMWP LLLGLSGVAALLQFFLLLLCPES PRYL IYIKLGKVEEAKKSLKRLRGNC DPMKEIAEMEKEKQEAASEKKVSIRQLFTSSKYKQAVIVA LMVQISQQFSGINAIFYSTNIFERAGVDQPVYATIGVGVVNTVFTVISVFLVEKAGRRSLFLA GLMGMLISAVAMTVGLALLSKFAWMSYVSMIAIFLVIFFEVGPGPIWPFIVAELFSQGPRPA AIATAGFCNWACNFIVGMCFQYIADLCGPYVFVIFAALLLIFFLFAYFKVPETKKGKSFEEIAAVF RRRKLPTKAMTELEDLRGREEA <i>NCBI Accession Number: MT472838</i>
GLUT3/SLC2A3	FLQKITTPLVYAVSIAAIGSLQFGYNTGVINAPEKIIQAFFNRTLSE RSGEVVSS ELLTSLWLSVA IFSVGGMIGSFSVSLFVNRFGRRRNSMLLVNILAFAGGVLMA LSKLVKAVEMLIVGRFIIIGFCG LSTGFVPMYISEVSPTSLRGAFGLTNQLGIVVGILVAQIFGLEAIMGTETLWPLLLGFTVLPVAVL QCVG LLLFCPESPRFLLINKVEE EKAQAVLQKLRGTEDVSQDIQEMKEESAKMSQEKKVTPEL FRSPSYRQAI IIAIMLQLSQQLSGINAVFYSTGIFERAGITKPVYATIGAGVNTVFTVVSLFLV ERAGRRTLHLVGLGGMALCTVLMTIALALRDSVEWIKYISIIATFGFVALFEIGPGPIWPFIVAE LFSQGPRPAAMAVAGCSNWTSNFLVGLLFPYAEKLLGSYVFLVFLVFLVIFVFTFFKVPETKG RTFEDI SRGFEGRGDASSPSPVEKVE LNSIEAEKVA <i>NCBI Accession Number: MT472839</i>
GLUT5/SLC2A5	M KLKGGKHESSDNDGSK GMTLT LALVALISAFGAS FQYGYNVSVINSPAPFMQE FYNQTY YRNGEYMSSEFQTL LWSLTVSMFPLGGLFGSLMVWPLVNNCGRKG TLLINNIFSIVA AVL M GTSEIAKTFEVIILSRVIMGIYAGLASNVVPMFLGELSPKNLRGAIGVVPQLFITVGILSAQILGL NSILGNAAGWPILLGLTGIPSL LQILLLPLFPESPRYLLIQKGNEEQARQALQRLRG CDDVYDEI EEMRREDESEKKEGQFSVLSLFTFRGLRWQLISII VMMMGQQLSGINAVFYADRFQ SAGV DTNSVQYVTVSIGAINVVM TLLAVFIIESLGRRI LLLAGFGLCCLSCAVLT LALNLQNTVTWMS YISIVCVIYIIGHAIGASPIPSVLITEMFLQSSRPAAFMVGGSVHWSNFTVGLLFLYMEAGLG PYSFLIFCAICLATIYIFIVVPETKNKTFMEINRIMAKRNKVEIQEDKDELKDFHTAPGGQAGKT VSSSEL <i>NCBI Accession Number: MT472840</i>

3.4 AIC Scores

Table S5: Akaike information criterion (AIC) and AIC with corrections for small sample size (AICc) scores presented for each GLUT isoform model. Due to a relatively small sample size, AICc was preferred over AIC. Models with the lowest AICc score were selected for post hoc analysis and are indicated with an asterisk (*). The models tested are as follows:

- 1: *Fluorescence Intensity* ~ *Treatment* + *Blot*
- 2: *Fluorescence Intensity* ~ *Tissue* + *Blot*
- 3: *Fluorescence Intensity* ~ *Treatment* + *Tissue* + *Blot*
- 4: *Fluorescence Intensity* ~ *Treatment* × *Tissue* + *Blot*

GLUT	Model	AIC Score	AICc Score	AIC Score	AICc Score
		WTH	WTH	PM	PM
GLUT1	1	515	519	31.9	34.4
	2	516	519	23.9	26.4
	3	479	485	25.2	29.2
	4	446	455*	17.4	23.4*
GLUT2	1	604	607	812	814
	2	570	575	773	776
	3	532	540	740	745
	4	462	478*	675	685*
GLUT3	1	270	273	373	375
	2	262	267	356	360
	3	238	246	341	346
	4	208	224*	308	318*
GLUT5	1	297	300	809	811
	2	278	283	770	773
	3	264	272	739	744
	4	234	250*	673	682*

3.5 Mammalian and Avian GLUT Homology

Table S6: Comparison of known avian GLUT isoforms and their homology to humans.

Data was aggregated from (M. S. Byers et al., 2017; Myrka & Welch, 2018; Sweazea & Braun, 2006; Kenneth C. Welch et al., 2013) and homology to humans was calculated using NCBI BLAST (Boratyn et al., 2012).

GLUT	Localisation	Feature	Chicken to hummingbird sequence homology	Chicken to human sequence homology	Hummingbird to human sequence homology	Substrates (mammals)
GLUT1	Ubiquitous	Basal glucose transport	98%	80%	88%	Glucose, galactose, mannose, glucosamine
GLUT2	Liver, Pancreas, Intestine, Kidney	Insulin dependent	89%	65%	64%	Fructose, Glucose, Galactose
GLUT3	Neurons, Liver, skeletal muscle	Insulin dependent	87%	70%	73%	Glucose
GLUT4	Not found	Absence	N/A	N/A	N/A	Glucose
GLUT5	Intestine, brain, adipocytes, testes, skeletal muscle	Fructose transport	81%	64%	66%	Fructose

Table S1: GLUTs 1, 2, 3, and 5 observed molecular weights in plasma membrane (PM) fractions and whole-tissue homogenates (WTH) of flight muscle, heart, and liver.

Representative immunoblots are shown for each tissue and fraction.

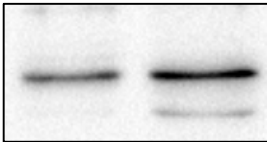
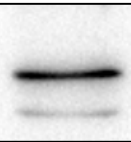
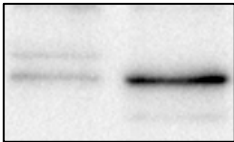
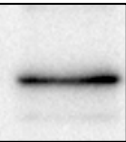
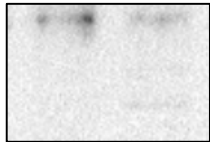
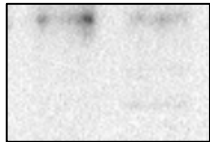
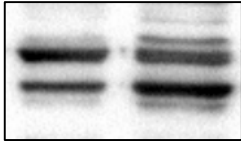
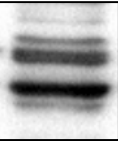
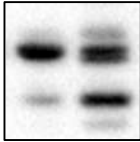

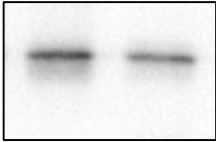
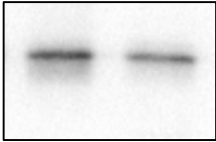
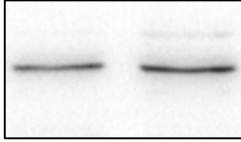
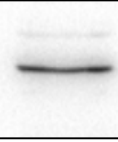
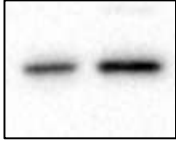

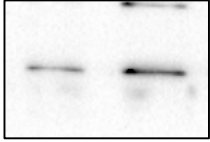
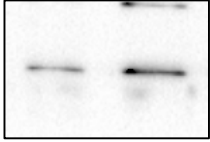
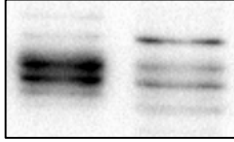
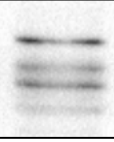
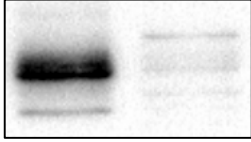
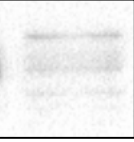
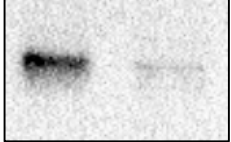
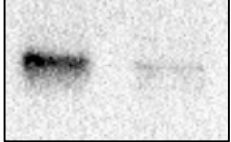
	Observed Molecular Weight	Flight Muscle		Heart		Liver	
		PMF	WTH	PMF	WTH	PMF	WTH
GLUT1 Predicted mW = 53.8 kDa	47.0 kDa →						
GLUT2 Predicted mW = 57.9 kDa	43.5 kDa →						
GLUT3 Predicted mW = 53.3 kDa	72.4 kDa →						
GLUT5 Predicted mW = 56.9 kDa	55.3 kDa →						

Table S2: Relative distribution of known cytosolic or PM-residing proteins following PM fractionation. Fraction purity indicates the relative abundance of protein in either the PM-only fraction compared to the without-PM-fraction (i.e. cytosolic proteins only).

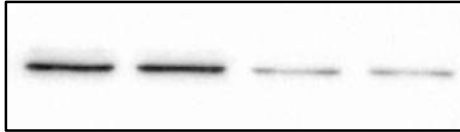
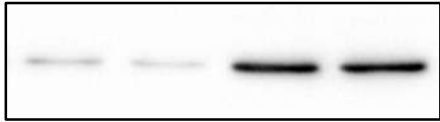
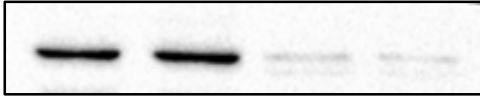
	Observed Molecular Weight	Plasma Membrane Fraction	Cytosolic Fraction (PM proteins removed)
E-Cadherin (PM-residing protein)	74.3kDa →		
	Fraction staining intensity:	92.1 ± 1.8 %	7.9 ± 1.8 %
GAPDH (cytosolic protein)	34.9 kDa →		
	Fraction staining intensity:	5.9 ± 0.5 %	94.1 ± 0.5 %
Na⁺/K⁺ ATPase (PM-residing protein)	103.1 kDa →		
	Fraction staining intensity:	92.1 ± 0.5 %	7.8 ± 0.5 %

Table S3: Immunoblots on lysates of overexpressed GLUT1, GLUT2, GLUT3, GLUT5 protein. Each immunoblot lane represents a cell lysate produced from an entire well of a 6-well cell-culture dish. Isoform specificity was tested via immunoblotting all cell lysates (empty vector control, acGLUT1, 2, 3, and 5) with each novel GLUT antibody and observing GLUT protein signal overlap. Anti-V5 tag represents targeted immunostaining of all GLUT protein expressed in that cell lysate. Black arrows refer to the band representing the GLUT protein isoform.

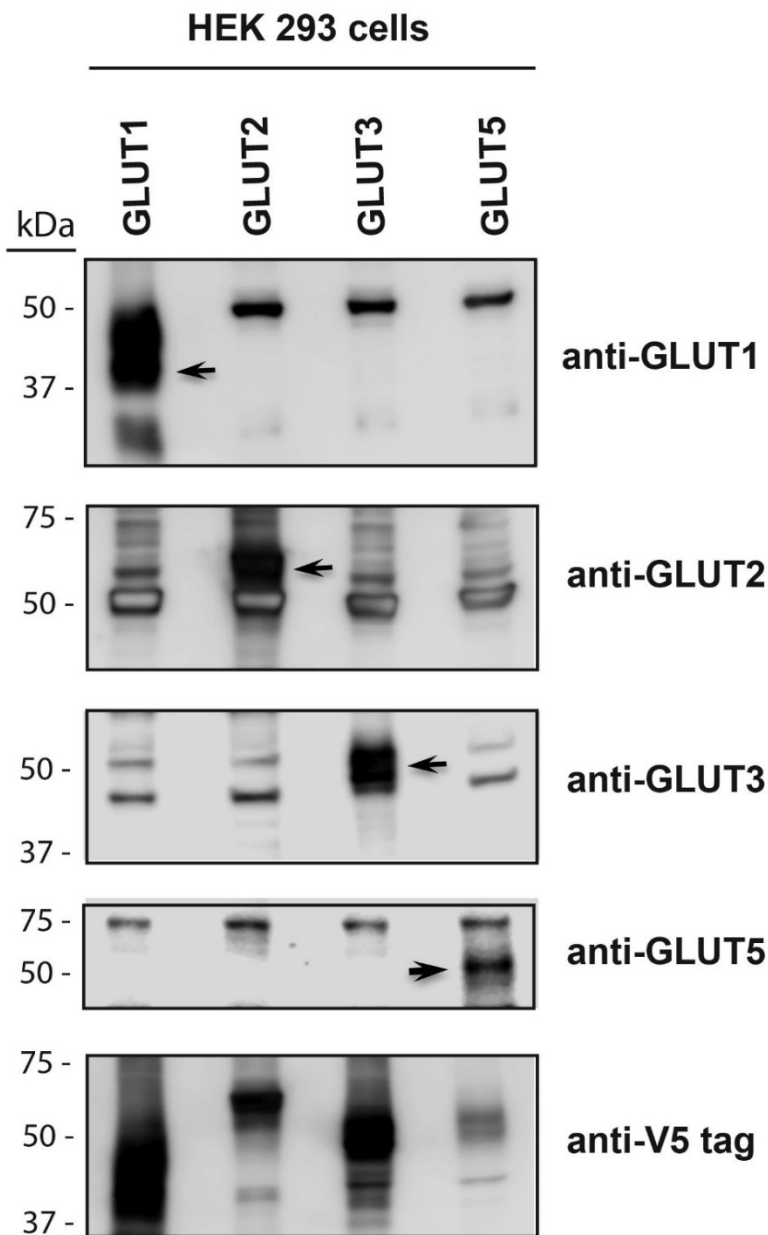


Table S4: Ruby-throated hummingbird specific GLUT1, GLUT2, GLUT3 and GLUT5 protein sequences. Highlighted regions indicated epitope targeted during antibody development to ensure greatest dissimilarity between targeted isoforms

Protein/Gene	Amino Acid Sequence
GLUT1/SLC2A1	METGSKMTARLMLAVGGAVLGSQFGYNTGVINAPQKVIEDFYNRTWLRYEETPITSATLTT LWLSVAIFSVGGMVGSFSVGLFVNRFGRNSMLMSNILAFLAAVLMGFSKMALSFEMLL GRFIIIGLYSGLTTGFVPMYVEVSPTALRGALGTFHQGLGIVLGILVAQVFLGLDLMGNDLWLP LLLGFIIVPALLQCIILPFAPESPRFLLINRNEENKAKSVLKKLRGTTDVSDDLQEMKEESRQMM REKKVTIMELFRSPMYRQPILIAIVLQLSQQLSGINAVFYSTSI FEKSGVEQPVYATIGSGVNT AFTVVSLFVVERAGRRTLHLIGLAGMAGCAVLMTIALTLDDQMPWMSYLSIVAIFGFVAFFEI GPGPIWPFIVAELFSQGPRPAFAVAGLSNWTSNFIVGMGFQYIAQLCGSYVFIIFTVLLILFFI FTYFKVPETKGRTFDEIA SGFRQGGAGQSDKTPDEFHS LGADSQV <i>NCBI Accession Number: MT472837</i>
GLUT2/SLC2A2	MDKKNKMQAEKHLTGLVLSVFAAVLGGFFQYGYSLGVINAPQKVEAHYGRVLIAPPDRFP TSASEEDGTPVTEPWWVSTEATLAPEDDPGEDLGTSSHILTMYSLSVSMFAVGGMVSSFT VGWIGDRLGRVKAMLVNNILSIIGNLLMGLAKFGPSHMLIIAGRAVTGLYCGLSGLVPMYVS EVSPTALRGALGTLHQLAIVTGILISQVLGLDFLLGNDEMWPPLLGLSGVAALLQFFLLLLCPES PRYLKILGKVEEAKKSLKRLRGNCNCPMKEIAEMEKEKQEAASEKKVSIRQLFTSSKYKQAVIVA LMVQISQQFSGINAIFYSTNIFERAGVDQPVYATIGVGVVNTVFTVISVFLVEKAGRRSLFLA GLMGMLISAVAMTVGLALLSKFAWMSYVSMIAIFLVIFFEVGPGPIWPFIVAELFSQGPRPA AIATAGFCNWACNFIVGMCFQYIADLCGPYVVFIFAALLLIFFLFAYFKVPETKKGKSFEEIAAVF RRRKLPTKAMTELEDLRGREEA <i>NCBI Accession Number: MT472838</i>
GLUT3/SLC2A3	FLQKITTPLVYAVSIAAIGSLQFGYNTGVINAPEKIIQAFFNRTLSESRGEVVSSELLTSLWLSVA IFSVGGMIGSFSVSLFVNRFGRNSMLLVNLAFAAGVLMALSKLVKAVEMLIVGRFIIIGIFCG LSTGFVPMYISEVSPTSLRGAFGLTNQLGIVVGILVAQIFGLEAIMGTETLWPLLLGFTVLPVL QCVGLLFCPESPRFLLINKVEEKAQAVLQKLRGTEDVSQDIQEMKEESAKMSQEKKVTPEL FRSPSYRQAIIIAIMLQLSQQLSGINAVFYSTGIFERAGITKPVYATIGAGVNTVFTVVSFLV ERAGRRTLHLVGLGGMALCTVLMTIALALRDSVEWIKYISIIATFGFVALFEIGPGPIWPFIVAE LFSQGPRPAAMAVAGCSNWTSNFLVGLLFPYAEKLLGSYVFLVFLVFLVIFVFTFFKVPETKG RTFEDI SRGFEGRGDASSPSPVEKVE LSNIEAEKVA <i>NCBI Accession Number: MT472839</i>
GLUT5/SLC2A5	M KLKGGKHESSDNDGSK GMTLTALVALISAFGASFGYGYNVSVINSPAPFMQEFYNQTY YRNGEYMSSEFQTLWLSLTVSMFPLGGLFGSLMVWPLVNNCGRKGTLINNIFSIVAAVLM GTSEIAKTFEVIILSRVIMGIYAGLASNVVPMFLGELSPKNLRGAIGVVPQLFITVGILSAQILGL NSILGNAAGWPILLGLTGIPSLQIILLPLFPESPRYLLIQKNEEQARQALQRLRGCDVYDEI EEMRREDESEKKEGQFSVLSLFTFRGLRWQLISIIVMMMGQQLSGINAVFYADRFQSGAV DTNSVQYVTVSIGAINVMTLLAVFIIESLGRRIILLAGFGLCCLSCAVLTALNLQNTVTWMS YISIVCVIYIIGHAIGASPIPSVLITEMFLQSSRPAAFMVGGSVHWSNFTVGLLFLYMEAGLG PYSFLIFCAICLATIYIFIVVPETKNKTFMEINRIMAKRNKVEIQEDKDELKDFHTAPGGQAGKT VSSSEL <i>NCBI Accession Number: MT472840</i>

Table S5: Akaike information criterion (AIC) and AIC with corrections for small sample size (AICc) scores presented for each GLUT isoform model. Due to a relatively small sample size, AICc was preferred over AIC. Models with the lowest AICc score were selected for post hoc analysis and are indicated with an asterisk (*). The models tested are as follows:

- 1: *Fluorescence Intensity* ~ *Treatment* + *Blot*
- 2: *Fluorescence Intensity* ~ *Tissue* + *Blot*
- 3: *Fluorescence Intensity* ~ *Treatment* + *Tissue* + *Blot*
- 4: *Fluorescence Intensity* ~ *Treatment* × *Tissue* + *Blot*

GLUT	Model	AIC Score	AICc Score	AIC Score	AICc Score
		WTH	WTH	PM	PM
GLUT1	1	515	519	31.9	34.4
	2	516	519	23.9	26.4
	3	479	485	25.2	29.2
	4	446	455*	17.4	23.4*
GLUT2	1	604	607	812	814
	2	570	575	773	776
	3	532	540	740	745
	4	462	478*	675	685*
GLUT3	1	270	273	373	375
	2	262	267	356	360
	3	238	246	341	346
	4	208	224*	308	318*
GLUT5	1	297	300	809	811
	2	278	283	770	773
	3	264	272	739	744
	4	234	250*	673	682*

Table S6: Comparison of known avian GLUT isoforms and their homology to humans.

Data was aggregated from (M. S. Byers et al., 2017; Myrka & Welch, 2018; Sweazea & Braun, 2006; Kenneth C. Welch et al., 2013) and homology to humans was calculated using NCBI BLAST (Boratyn et al., 2012).

GLUT	Localisation	Feature	Chicken to hummingbird sequence homology	Chicken to human sequence homology	Hummingbird to human sequence homology	Substrates (mammals)
GLUT1	Ubiquitous	Basal glucose transport	98%	80%	88%	Glucose, galactose, mannose, glucosamine
GLUT2	Liver, Pancreas, Intestine, Kidney	Insulin dependent	89%	65%	64%	Fructose, Glucose, Galactose
GLUT3	Neurons, Liver, skeletal muscle	Insulin dependent	87%	70%	73%	Glucose
GLUT4	Not found	Absence	N/A	N/A	N/A	Glucose
GLUT5	Intestine, brain, adipocytes, testes, skeletal muscle	Fructose transport	81%	64%	66%	Fructose

Figure S1: Representative immunoblots for relative whole-tissue abundance of GLUT1, GLUT2, GLUT3, and GLUT5 in flight muscle, heart, and liver of fed and fasted hummingbirds. Immunoblots are presented here for whole tissue homogenates of hummingbird tissue. Observed molecular weights (M.W.) are reported.

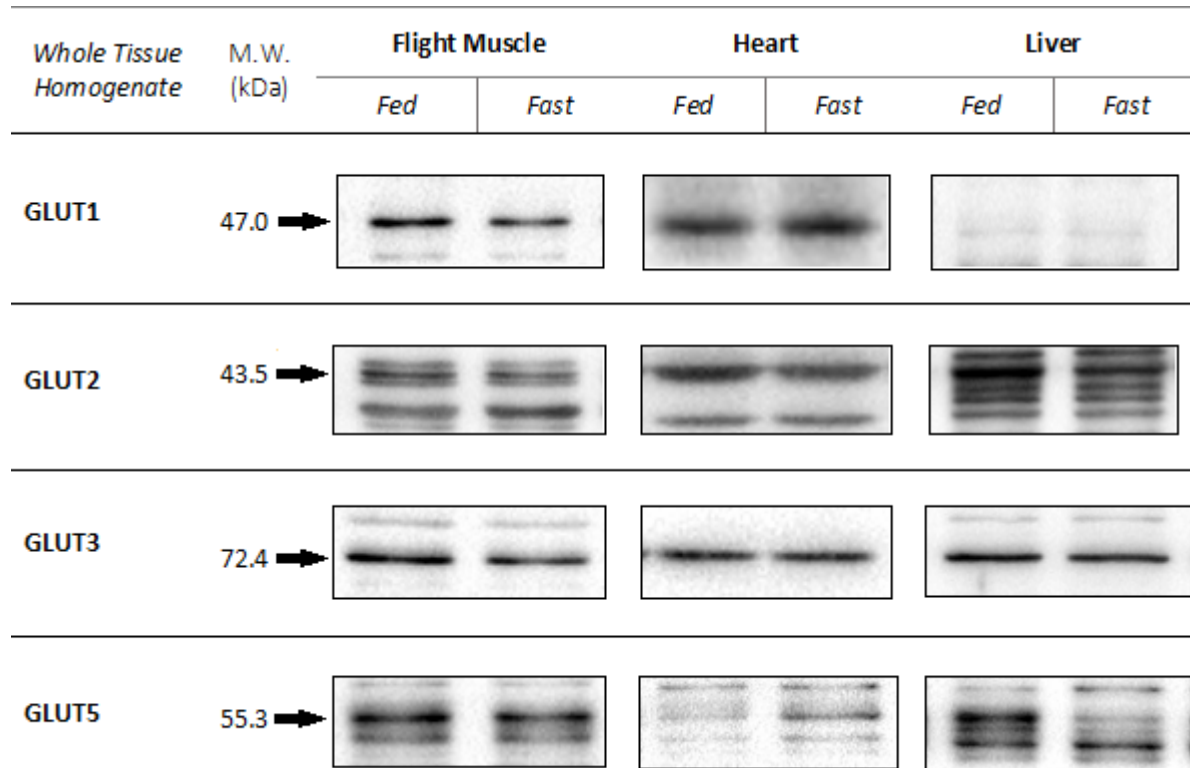


Figure S2: Representative immunoblots for relative PM abundance of GLUT1, GLUT2, GLUT3, and GLUT5 in flight muscle, heart, and liver of fed and fasted hummingbirds. Immunoblots are presented here for hummingbird tissue samples that underwent plasma membrane fractionation; only PM-residing GLUTs are presented. Observed molecular weights (M.W.) are reported.

